

Spectral identification and estimation of mixed causal-noncausal invertible-noninvertible models

Alain Hecq* and Daniel Velasquez-Gaviria†

Maastricht University

October 31, 2023

Abstract

This paper introduces new techniques for estimating, identifying and simulating mixed causal-noncausal invertible-noninvertible models. We propose a framework that integrates high-order cumulants, merging both the spectrum and bispectrum into a single estimation function. The model that most adequately represents the data under the assumption that the error term is i.i.d. is selected. Our Monte Carlo study reveals unbiased parameter estimates and a high frequency with which correct models are identified. We illustrate our strategy through an empirical analysis of returns from 24 Fama-French emerging market stock portfolios. The findings suggest that each portfolio displays noncausal dynamics, producing white noise residuals devoid of conditional heteroscedastic effects.

Keywords: Noncausal, Noninvertible, High-order cumulants, Spectrum, Bispectrum, Heteroscedasticity.

MSC code: 91B84, 91G80, 91G60.

JEL code: C510, C530, C580, C140.

1 Introduction

Econometricians have traditionally considered $ARMA(p, q)$ models using the Box-Jenkins methodology to describe and forecast time series. This method heavily rely on the assumption that the autoregressive (AR) and moving average (MA) components should be respectively causal and invertible. This essentially means that the roots of both AR and MA polynomials are situated outside the unit circle on the complex plane, which guarantees that the model converges to a unique, stable solution. Instead, non-causal and non-invertible models have their respective roots located within the unit circle. The increasing interest in these models comes from their adeptness at capturing complex non-linear phenomena such as bubbles and asymmetric cycles. This capacity to reflect anticipation and speculation resonates strongly with observable behaviors in financial markets (Lanne and Saikkonen (2011), Hecq, Lieb, and Telg (2016); Hecq and Velasquez-Gaviria (2022); Hecq and Voisin (2019); Lof (2013); Lof and Nyberg (2017), Gouriéroux and Zakoïan (2017)).

*a.hecq@maastrichtuniversity.nl, Maastricht University, SBE, Department of Quantitative Economics, P.O.Box 616, 6200 MD Maastricht, The Netherlands.

†Corresponding author: d.velasquezgaviria@maastrichtuniversity.nl, Maastricht University, SBE, Department of Quantitative Economics, P.O.Box 616, 6200 MD Maastricht, The Netherlands.

The interpretation of noncausal and noninvertible models owes a lot to the literature looking at non-fundamental solutions within expectation frameworks, suggesting that expectations can significantly influence present-day prices. In [Fama \(1970\)](#); [Fischer \(1977\)](#); [Lucas Jr \(1972\)](#); [Muth \(1961\)](#), within the paradigm of the rational expectations hypothesis, agents judiciously harness all accessible information when making consumption and investment decisions. This includes forecasts about prospective events. A comprehensive understanding of how future information affects current prices emerges from [Hansen, Sargent, et al. \(1991\)](#). The main argument is the disparity between the breadth of information available to agents versus econometricians, advocating for the incorporation of future values, or at the very least, expectations of such values, to bolster the precision of models. In [Diba and Grossman \(1988\)](#)'s "rational bubble" framework stock prices are not solely anchored to conventional market indicators such as anticipated dividends but also by elements not rooted in market fundamentals. In feedback loop models (see [Shiller, Fischer, and Friedman \(1984\)](#)) traders that are foreseeing an uptick in a stock's value, may engage in contemporary buying sprees.

To emulate such intricate behaviors, we identify and estimate mixed autoregressive causal-noncausal invertible-noninvertible moving average model, denoted as $MARMA(r, s, r', s')$. This model decomposes the $AR(p)$ and $MA(q)$ polynomials based on the positioning of their roots relative to the unit circle. The outcome is a refined ARMA model, which considers both lags and leads of the endogenous variable, where the relationship $p = r + s$. Furthermore, this model incorporates both past (retrospective) and future (anticipatory) errors, represented by the equation $q = r' + s'$. MARMA models have a unique and stationary solution ([Brockwell and Davis \(1987\)](#) (p. 81)). Notably, this deviates from the nonstationary solutions where the endogenous variable remains contemporaneously uncorrelated with its error sequence. Traditional estimation techniques, grounded in Gaussianity or second-order moments, fail to pinpoint this stationary solution. This stems from the fact that both causal (invertible) and noncausal (noninvertible) processes exhibit identical autocorrelation functions and spectral densities. Therefore, the resultant estimated coefficients predominantly have roots outside the unit circle, disregarding the possibility that the true process structure might possess roots within the unit circle. Indeed, an $ARMA(p, q)$ model has 2^{p+q} parameter configurations with identical probability structures ([Rosenblatt \(2012\)](#)). However, when the error term follows a non-Gaussian distribution, each of the 2^{p+q} process is distinctly identifiable within a $MARMA(r, s, r', s')$ representation ([Wu and Davis \(2010\)](#)). The repercussions for an econometrician's misstep in estimating a time series that potentially integrates noncausal or noninvertible dynamics using traditional ARMA models can have important modelling consequences. As such one can get spurious higher-order dependencies in the conditional moments of errors, which is akin to conditional heteroscedasticity (manifesting as GARCH-type effects; see [Gouriéroux, Zakoian, et al. \(2013\)](#), proposition 3), [Rosenblatt \(2000\)](#); [Velasco \(2022\)](#)).

Most literature on MAR (and MARMA) gravitates towards the Maximum Likelihood estimator when exploring error sequences that are both i.i.d and non-Gaussian ([Bredt, Davis, Lh, and Rosenblatt \(1991\)](#); [Hecq et al. \(2016\)](#); [Huang and Pawitan \(2000\)](#); [Lanne and Saikkonen \(2011\)](#); [K. Lii and Rosenblatt \(1982\)](#); [K.-S. Lii and Rosenblatt \(1992, 1996\)](#); [Meitz and Saikkonen \(2013\)](#)). MLE boasts consistency across symmetric, strictly positive, and smooth non-Gaussian probability density functions. Yet, empirical situations often lack prior knowledge of distribution functions. Any arbitrary choice in this context can potentially introduce biases in parameters and erroneous model identification. Our paper offers an innovative approach by sidestepping this requirement. Instead, we advocate a spectral domain strategy using higher-order cumulants and spectral densities within a least squares framework. Our method hinges on the minimum distance estimation between the second and third-order spectral densities (namely, the spectrum and bispectrum). Using the frequency domain representation of the data via the periodogram and biperiodogram, we minimize the second and third-order dependence, aligning with the white

noise and i.i.d premises, moreover obtaining error sequences that do not exhibit heteroscedastic effects. Note that [Rosenblatt \(1980\)](#) already recommended an amalgamation of both the spectrum and bispectrum when considering ARMA models with roots outside or within the unit circle. See also [K. Lii and Rosenblatt \(1982\)](#), [Kumon \(1992\)](#) and [Brillinger \(1985\)](#) for higher-order spectral methodologies. Closer to our paper, [Velasco and Lobato \(2018\)](#) incorporate spectral densities and periodograms exceeding the third order into the estimation matrix of potential noncausal and noninvertible ARMA processes. See also [Lobato and Velasco \(2022\)](#) for non-stationary fractional integrated ARMA process models.

Our paper presents several contributions to the study of MARMA models. We first introduce a variation of the estimation method proposed in [Velasco and Lobato \(2018\)](#). We modify the transfer function to distinguish between the polynomials with roots inside and outside the unit circle, tailored for MARMA models. This draws a clear distinction between causal-noncausal and invertible-noninvertible polynomials, a strategy reminiscent of [K.-S. Lii and Rosenblatt \(1996\)](#). [Hecq and Velasquez-Gaviria \(2022\)](#) observed a pronounced reliance on initial values. To remedy this, our current approach directly targets parameter estimation using Genetic Algorithms rather than their root-based factorization, significantly reducing dependence on initial values. The advantage of using Genetic Algorithms is that by simulating the evolutionary process, they explore a vast parameter space, rendering initial values irrelevant and enhancing the likelihood of finding the global minimum of the target function.

Notably, our refined estimator’s consistency and asymptotic normality mirror those of its predecessor. Secondly, we develop an identification of the MARMA model based on the existence of the global minimum of our estimation function. This minimum remains consistent, provided the second and third-order cumulants are present. Our third contribution is an alternative method to simulate MARMA processes in the frequency domain. We exploit the inverse Fourier transform of the error sequence combined with the model’s transfer function, ensuring streamlined replication. Our fourth contribution is the study of the monthly returns across 24 Fama-French portfolios in emerging markets. Drawing a parallel to [Gospodinov and Ng \(2015\)](#), which unearthed a noninvertible MA(0,1) model across 25 similarly curated portfolios in developed markets, our findings reveal a mosaic of noncausal and mixed causal-noncausal dynamics. To test the validity of the i.i.d property on our derived residuals, we deploy statistical tools proposed by [Dalla, Giraitis, and Phillips \(2020\)](#). We consistently obtain error sequences devoid of heteroscedastic effects under our identified and estimated noncausal dynamics.

The paper is divided as follows: Section 2 presents our methodology. Section 3 delves deep into spectral estimation. Section 4 introduces i.i.d tests. Section 5 delineates our MARMA model simulation procedure. Sections 6 and 7, respectively, showcase the insights from our Monte Carlo analysis and the empirical application. The final section concludes.

2 Methodology

2.1 ARMA(p, q) model

The zero mean (for the simplicity of the presentation) stationary time series y_t for every $t = \{0, \pm 1, \pm 2, \pm 3, \dots\}$ with length T and $\mathbb{E}[y_t^2] < \infty$, is said to be an ARMA(p, q) process if it satisfies the recursion

$$y_t - \phi_1 y_{t-1} - \dots - \phi_p y_{t-p} = \epsilon_t + \theta_1 \epsilon_{t-1} + \dots + \theta_q \epsilon_{t-q}, \quad (1)$$

where $\epsilon_t \sim \text{WN}(0, \sigma^2)$ is white noise. Note that this definition only considers the first two moments of ϵ_t . Equation 1 can be written in a compact form as

$$\phi(L)y_t = \theta(L)\epsilon_t, \quad (2)$$

where L is the backward shift operator, that is, $L^\ell = y_{t-\ell}$ for $\ell = \{0, \pm 1, \pm 2, \pm 3, \dots\}$, $\phi(L)$ is a p -th order autoregressive (AR) polynomial, and $\theta(L)$ is a q -th order moving-average (MA) polynomial. Both polynomials can be expressed in terms of their roots as

$$\phi(z) = 1 - \phi_1 z - \dots - \phi_p z^p, \quad \text{and} \quad \theta(z) = 1 + \theta_1 z + \dots + \theta_q z^q, \quad (3)$$

where $\phi(z)$ and $\theta(z)$ have no common roots, and all of their roots are outside the unit circle, that is $\phi(z) \neq 0$ for $|z| < 1$, and $\theta(z) \neq 0$ for $|z| < 1$. Therefore, there exists a unique and strictly stationary solution of ARMA(p, q), determining that the model is causal and invertible. The ARMA(p, q) model is causal if there exists a sequence of constants $\{\pi_j\}$, such that

$$y_t = \sum_{j=0}^{\infty} \pi_j \epsilon_{t-j}, \quad (4)$$

with $\sum_0^\infty |\pi_j| < \infty$ and y_t expressed in terms of the present and past of the errors sequence that is an MA(∞). On the other hand, the ARMA(p, q) model is invertible if there exists a sequence of constants $\{\pi_j^*\}$, such that

$$\epsilon_t = \sum_{j=0}^{\infty} \pi_j^* y_{t-j}, \quad (5)$$

with when $\sum_{j=0}^\infty |\pi_j^*| < \infty$, ϵ_t is formulated in terms of both the present and historical values of y_t , effectively characterizing it as an AR(∞) process. The nature of the ARMA(p, q) model is determined by the roots of the polynomials $\phi(z)$ and $\theta(z)$. Specifically, if the roots of $\phi(z)$ lie within the unit circle, the model is categorized as noncausal. Conversely, the presence of the roots of $\theta(z)$ within the unit circle designates the model as noninvertible.

For time series where y_t adheres to Gaussian properties, its entire probability framework is anchored to its autocovariance function, see [K.-S. Lii and Rosenblatt \(1996\)](#). A consequence of this property is the existence of 2^{p+q} distinct models, each formulated from different parameter combinations, yet sharing an identical autocovariance function. This overlap obfuscates the differentiation between noncausal and noninvertible models; second-order estimators invariably converge to their causal and invertible analogs. As a result, it has become a prevailing practice among econometricians to sidestep noncausal and noninvertible models, especially given that no substantial insights are forsaken from a second-order viewpoint, as discussed in [Brockwell and Davis \(1987\)](#), p. 81. However, in the context of non-Gaussian y_t , each model manifests with a distinct probability structure, facilitating the discernment and identification of noncausal and noninvertible models when they emerge. Such precision invariably leads to an enhanced data representation, as elaborated by [Wu and Davis \(2010\)](#).

2.2 MARMA(r, s, r', s') model

The ARMA(p, q) model can be extended to obtain the mixed causal-noncausal and invertible-noninvertible process, namely the MARMA(r, s, r', s') model

$$(1 - \phi_1^+ L - \dots - \phi_r^+ L^r)(1 - \phi_1^* L^{-1} - \dots - \phi_s^* L^{-s})y_t = (1 + \theta_1^+ L + \dots + \theta_r^+ L^{r'}) (1 + \theta_1^* L^{-1} + \dots + \theta_{s'}^* L^{-s'}) \epsilon_t, \quad (6)$$

where $\epsilon_t \stackrel{\text{i.i.d.}}{\sim} \mathfrak{G}(\zeta)$ with \mathfrak{G} a distribution function and ζ its parameters. The first three moments/cumulants are denoted

$$\mathbb{E}(\varepsilon_t) = 0, \quad \mathbb{E}(\varepsilon_t^2) = \kappa_2^*, \quad \mathbb{E}(\varepsilon_t^3) = \kappa_3^*. \quad (7)$$

Moreover, ε_t has bounded moments of order k , with $k \geq 3$. Note that in the traditional ARMA model, ε_t is white noise, implying that all higher-order properties of its joint distribution are ignored, except for its first and second moments, $E(\varepsilon_t)$ and $E(\varepsilon_t \varepsilon_s)$. On the other hand, ε_t is i.i.d, implying independence in its high-order moments. Equation 6 can be expressed in terms of its decomposed polynomials as

$$\begin{aligned} \phi(z) &= \phi^+(z)\phi^*(z) = (1 - \phi_1^+ z - \dots - \phi_r^+ z^r)(1 - \phi_1^* z - \dots - \phi_s^* z^s), \\ \theta(z) &= \theta^+(z)\theta^*(z) = (1 + \theta_1^+ z + \dots + \theta_{r'}^+ z^{r'})(1 + \theta_1^* z - \dots - \theta_{s'}^* z^{s'}). \end{aligned} \quad (8)$$

The polynomials $\phi^+(z)$, $\phi^*(z)$, $\theta^+(z)$, and $\theta^*(z)$ have no common roots and are different from zero. $\phi^+(z)$ is a r -th order polynomial, $\phi^*(z)$ is a s -th order polynomial, $\theta^+(z)$ is a r' -th order polynomial, and $\theta^*(z)$ is a s' -th polynomial. The order of the polynomials $\phi(z)$ and $\theta(z)$ are $p = r + s$ and $q = r' + s'$. The polynomials $\phi^+(z)$ and $\theta^+(z)$ have their zeros outside the unit circle. In contrast, the polynomials $\phi^*(z)$, and $\theta^*(z)$ have their zeros inside the unit circle, that is

$$\begin{aligned} \phi^+(z) &\neq 0 \text{ for } |z| < 1 \quad \text{and} \quad \theta^+(z) \neq 0 \text{ for } |z| < 1, \\ \phi^*(z) &\neq 0 \text{ for } |z| > 1 \quad \text{and} \quad \theta^*(z) \neq 0 \text{ for } |z| > 1. \end{aligned} \quad (9)$$

In Equation 9, we exclude the unit root case for convenience. Note that the noncausal component allows a forward-looking representation of y_t . Similarly, the noninvertible component allows the forward-looking representation of ε_t . The MARMA(r, s, r', s') is represented as

$$\phi^+(z)\phi^*(z)y_t = \theta^+(z)\theta^*(z)\varepsilon_t. \quad (10)$$

Note that our presentation of the model is similar to [K.-S. Lii and Rosenblatt \(1992\)](#) Equation (1.2), and [Fries \(2021\)](#). Similar representations can be seen for the MA component in [Meitz and Saikkonen \(2013\)](#); [Nyholm et al. \(2019\)](#), and for the AR component in [Hecq et al. \(2016\)](#); [Lanne and Saikkonen \(2011\)](#). Under these conditions, the inverses of the lag polynomials are

$$\begin{aligned} \phi^+(z)^{-1} &= \sum_{j=0}^{\infty} \alpha_j z^j, \quad \phi^*(z)^{-1} = \sum_{j=s}^{\infty} \beta_j z^{-j}, \\ \theta^+(z)^{-1} &= \sum_{j=0}^{\infty} \alpha'_j z^j, \quad \theta^*(z)^{-1} = \sum_{j=s'}^{\infty} \beta'_j z^{-j}. \end{aligned} \quad (11)$$

The random variables z_t are assumed to have a density function $f_\sigma(z) = \frac{1}{\sigma} f(\frac{z}{\sigma})$. Given these representations, the MARMA(r, s, r', s') model has a unique and stationary solution, admitting a two-sided representation, an MA(∞), and an AR(∞), see Theorem 3.1.3 in [Brockwell and Davis \(1987\)](#). The MA(∞) representation as

$$y_t = \sum_{j=-\infty}^{\infty} \Psi_j \varepsilon_{t+j}, \quad \text{where} \quad \frac{\theta^+(z)\theta^*(z)}{\phi^+(z)\phi^*(z)} \stackrel{\text{def}}{=} \sum_{j=-\infty}^{\infty} \Psi_j z^j = \Psi(z), \quad (12)$$

where Ψ_j are the coefficient of z^j in the Laurent expansion of $\frac{\theta^+(z)\theta^*(z)}{\phi^+(z)\phi^*(z)} \stackrel{\text{def}}{=} \Psi(z)$. Note that $\Psi(z)$ is absolute convergent in the annulus $D = \{z : \delta < |z| < \delta^{-1}\}$, $\delta < 1$, see Example 1, in [Breidt and Davis \(1992\)](#). Also, the coefficients Ψ_j geometrically decay to zero as $j \rightarrow \infty$. Similarly, ε_t can be expressed in terms of y_t in an AR(∞) representation as

$$\varepsilon_t = \sum_{j=-\infty}^{\infty} \Psi_j^* y_{t+j}, \quad \text{where} \quad \frac{\phi^+(z)\phi^*(z)}{\theta^+(z)\theta^*(z)} = \sum_{j=-\infty}^{\infty} \Psi_j^* z^j = \Psi^*(z), \quad (13)$$

where Ψ_j^* is the coefficient of z^j in the Laurent expansion of $\frac{\phi^+(z)\phi^*(z)}{\theta^+(z)\theta^*(z)} \stackrel{\text{def}}{=} \Psi^*(z)$. $\Psi^*(z)$ is absolute convergent in some annulus $D = \{z : \delta < |z| < \delta^{-1}\}, \delta < 1$. The coefficients Ψ_j^* geometrically decay to zero as $j \rightarrow \infty$. Note that from the MARMA model can emerge the causal and noncausal AR model, the invertible and noninvertible MA, and the mixed causal-noncausal and mixed invertible-noninvertible, as follows in Remark 1.

Remark 1. Particular cases of the MARMA(r, s, r', s') model are

1. If $\phi^*(z) \equiv \theta^+(z) \equiv \theta^*(z) \equiv 1$, the resulting model is a purely causal MAR($r, 0$).
2. If $\phi^+(z) \equiv \theta^+(z) \equiv \theta^*(z) \equiv 1$, the resulting model is a purely noncausal MAR($0, s$).
3. If $\phi^+(z) \equiv \phi^*(z) \equiv \theta^*(z) \equiv 1$, the resulting model is an invertible MA($r', 0$).
4. If $\phi^+(z) \equiv \phi^*(z) \equiv \theta^+(z) \equiv 1$, the resulting model is a noninvertible MA($0, s'$).
5. If $\theta^+(z) \equiv \theta^*(z) \equiv 1$, the resulting model is a mixed causal-noncausal MAR(r, s).
6. If $\phi^+(z) \equiv \phi^*(z) \equiv 1$, the resulting model is a mixed invertible-noninvertible MMA(r', s').

For the estimation of the MARMA(r, s, r', s') model, it is convenient to denote the set of parameters as

$$\vartheta = (\phi_1^+, \dots, \phi_r^+, \phi_1^*, \dots, \phi_s^*, \theta_1^+, \dots, \theta_{r'}^+, \theta_1^*, \dots, \theta_{s'}^*). \quad (14)$$

2.3 Spectral representation of the MARMA(r, s, r', s') process

This section defines the spectrum for the MARMA(r, s, r', s') process. We provide the theory and the intuition to decompose the MARMA process into periodic components that appear in proportion to their variance (second-order cumulant) and higher-order moments/cumulants in the case of the bispectrum. Let us assume y_t be a stationary process with an autocovariance function

$$\kappa_2(j) = \mathbb{E}[y_t y_{t-j}], \quad \text{for } j = \{0, \pm 1, \pm 2, \pm 3, \dots\}. \quad (15)$$

The autocovariance function is absolute summable $\sum_{-\infty}^{\infty} |\kappa_2(j)| < \infty$. Therefore, there exists a unique monotonically increasing function $S_2(\omega)$, called the spectrum, with $S_2(-\infty) = S_2(-1/2) = 0$, and $S_2(\infty) = S_2(1/2) = \kappa_2(0)$, as

$$\kappa_2(j) = \int_{-\pi}^{\pi} S_2(\omega) e^{-ij\omega} d\omega, \quad (16)$$

where $\omega = 2\pi/T$ is the Fourier frequency, and i is the imaginary number. The autocovariance considers linear relations of the data in two time periods, known as second-order dependence, also that $\kappa_{2j} = \kappa_{2j-1} \dots = \kappa_{2j-n} = \kappa_{2j+1} \dots = \kappa_{2j+n}$. In any of these representations, the autocovariance functions remain unchanged. We obtain the spectrum by the inverse transform of Equation 16, as

$$S_2(\omega_j) = \frac{1}{2\pi} \sum_{j=-\infty}^{\infty} \kappa_2(j) e^{-ij\omega}. \quad (17)$$

The spectrum and the autocovariance function contain the same information, although expressed in different ways. The autocovariance expresses the dependence between leads or lags, and the spectrum expresses it in cycles,

determined by the Fourier frequencies. Of particular interest is the spectrum of the error sequence ε_t . Since its autocovariance function is

$$\kappa_2^*(j) = \begin{cases} \kappa_2^* & j = 0 \\ 0 & j \neq 0 \end{cases}. \quad (18)$$

The spectrum of ε_t is $S_2^\varepsilon = \kappa_2^*$, that is a constant value for all frequencies.

When y_t is non-Gaussian, its probability structure depends not only on its autocovariance function but also on the higher-order moments. We specify that the first three moments are equivalent to the first three cumulants, which is not valid for cumulants of order greater than three. In particular, the third cumulant contains the relations of the time series at three points in time. Hence it is known as the triple correlation function or the bicoariance function, see [Bartelt, Lohmann, and Wirnitzer \(1984\)](#). The third order cumulant is

$$\kappa_3(j, l) = \mathbb{E}[y_t y_{t-j} y_{t-l}], \quad \text{for } j, l = \{0, \pm 1, \pm 2, \pm 3, \dots\}. \quad (19)$$

Note that $\kappa_3(j, l)$ is equal to zero for the Gaussian distribution. $\kappa_3(j, l)$ satisfies the following symmetries

$$\kappa_3(j, l) = \kappa_3(l, j) = \kappa_3(-j, l - j) = \kappa_3(l - j, -j) = \kappa_3(j - l, -l) = \kappa_3(-l, j - l). \quad (20)$$

Like the spectrum, the bispectrum is the frequency domain tool for representing non-Gaussian relations. We define the spectrum in terms of the bicoariance function as

$$\kappa_3(j, l) = \int_{-\pi}^{\pi} \int_{-\pi}^{\pi} S_3(\omega_1, \omega_2) e^{-i(j\omega_1 + l\omega_2)} d\omega_1 d\omega_2. \quad (21)$$

We obtain the bispectrum by the inverse transform of Equation 21, as

$$S_3(\omega_1, \omega_2) = \frac{1}{(2\pi)^2} \sum_{j=-\infty}^{\infty} \sum_{l=-\infty}^{\infty} \kappa_3(j, l) e^{-i(j\omega_1 + l\omega_2)}. \quad (22)$$

For errors sequence ε_t , the bicoariance function is

$$\kappa_3^*(j, l) = \mathbb{E}[\varepsilon_t \varepsilon_{t-j} \varepsilon_{t-l}], \quad (23)$$

Thus, the bispectrum of ε_t is $S_3^\varepsilon = \kappa_3^*(j, l)$. Using this information, we can formulate the spectrum of the MARMA(r, s, r', s') model. The linear filter from Equation 12 is the convolution of the error sequence ε_t into y_t . Then, we can define the frequency impulse response function or transfer function as

$$\psi(\boldsymbol{\vartheta}, \omega) = \sum_{j=-\infty}^{\infty} \Psi_j e^{-ij\omega} = \frac{(1 + \theta_1^+ z + \dots + \theta_r^+ z^r)(1 + \theta_1^* z + \dots + \theta_{s'}^* z^{s'})}{(1 - \phi_1^+ z - \dots - \phi_r^+ z^r)(1 - \phi_1^* z - \dots - \phi_s^* z^s)}, \quad (24)$$

where $z = e^{-i\omega}$. Note that in [Hecq and Velasquez-Gaviria \(2022\)](#) the numerator of the Equation 24 is equal to one, since they ignore the MA component. In this way, using the spectral density of ε_t , it is possible to deduce the spectral density of y_t as

$$S_2(\boldsymbol{\vartheta}, \omega) = \frac{\kappa_2^*}{2\pi} \psi(\boldsymbol{\vartheta}, \omega) \overline{\psi(\boldsymbol{\vartheta}, \omega)} = \frac{\kappa_2^*}{2\pi} |\psi(\boldsymbol{\vartheta}, \omega)|^2, \quad (25)$$

where $\overline{\psi(\boldsymbol{\vartheta}, \omega)}$, is the conjugate of the transfer function. In the same fashion, the bispectrum of y_t is

$$S_3(\boldsymbol{\vartheta}, \omega_1, \omega_2) = \frac{\kappa_3^*}{4\pi^2} \psi(\boldsymbol{\vartheta}, \omega_1) \psi(\boldsymbol{\vartheta}, \omega_2) \overline{\psi(\boldsymbol{\vartheta}, -\omega_1 - \omega_2)}, \quad (26)$$

where $\overline{\psi(\boldsymbol{\vartheta}, -\omega_1 - \omega_2)}$ is the complex conjugate of the transfer function, evaluated at the sum of frequencies ω_1 and ω_2 .

3 Spectral estimation

3.1 Spectrum and bispectrum

The nonparametric estimation of the spectrum and bispectrum for autoregressive processes is usually based on methods employing the discrete Fourier transform (DFT)

$$d_T(\omega) = \sum_{t=1}^T y_t e^{-it\omega}. \quad (27)$$

The most popular estimator for the spectrum is the periodogram. For a summary of estimates of the spectrum, see [Kay and Marple \(1981\)](#). The periodogram is obtained as the modulus of the output values from the DFT in Equation 27, performed directly on the time series. The periodogram has been widely used in spectral analysis and autoregressive modeling, see [Alekssev \(1996\)](#); [Bartlett \(1950\)](#); [Brillinger \(1975\)](#); [Brillinger and Rosenblatt \(1967\)](#); [Rosenblatt \(1965\)](#). The periodogram is defined as

$$I_2(\omega) = \frac{1}{2\pi T} d_T(\omega) \overline{d_T(\omega)}. \quad (28)$$

Similar to the periodogram, taking into account relations between three frequencies (bifrequencies), the biperiodogram is the bispectrum estimator, defined as

$$I_3 = (\omega_1, \omega_2) = \frac{1}{(2\pi)^2 T} d_T(\omega_1) d_T(\omega_2) \overline{d_T(-\omega_1 - \omega_2)}, \quad (29)$$

where $\overline{d_T(-\omega_1 - \omega_2)}$, represents the complex conjugate of the Fourier transform of the sum of two frequencies, accounting for the asymmetries present in the non-Gaussian data. Note that the biperiodogram is a complex quantity due to its last factor of the sum of frequencies. The periodogram and biperiodogram are asymptotically unbiased estimators of the spectrum and bispectrum but inconsistent. For details see [Alekssev \(1996\)](#); [Brillinger \(1975\)](#); [Rosenblatt \(1965\)](#). Some properties of the periodogram are developed in [Brillinger and Rosenblatt \(1967\)](#); in particular, the mean, the standard deviation, and its correlation between frequencies.

We employ the estimation function proposed by [Velasco and Lobato \(2018\)](#). We first perform a preliminary Gaussian likelihood estimation and obtain $\bar{\boldsymbol{\vartheta}}$, assuming the model is causal and invertible. We evaluate the second order estimates in the transfer functions $\psi(\bar{\boldsymbol{\vartheta}}, \omega)$, $\psi(\bar{\boldsymbol{\vartheta}}, -\omega_i - \omega_j)$ and the second order cumulant $\bar{\kappa}_2$. This normalization by preliminary estimates has no effect on the identification of the parameters since they are invariant to any inversion of the polynomial roots and significantly simplifies the estimation compared with [Leonenko, Sikorskii, and Terdik \(1998\)](#). The estimation function is

$$R_T(\boldsymbol{\vartheta}) = A_{2T} \sum_{j=1}^{T-1} \left(\frac{I_2(\omega_j) - S_2^*(\boldsymbol{\vartheta}, \omega_j)}{\psi(\bar{\boldsymbol{\vartheta}}, \omega_j) \psi(\bar{\boldsymbol{\vartheta}}, -\omega_j)} \right)^2 + A_{3T} \sum_{j=1}^{T-1} \sum_{i=1}^{T-1} \frac{|I_3(\omega_j, \omega_i) - S_3^*(\boldsymbol{\vartheta}, \omega_j, \omega_i)|^2}{\psi(\bar{\boldsymbol{\vartheta}}, \omega_j) \psi(\bar{\boldsymbol{\vartheta}}, \omega_i) \psi(\bar{\boldsymbol{\vartheta}}, -\omega_j - \omega_i)}, \quad (30)$$

where $A_{2T} = m(2\pi)^2 / (4\bar{\kappa}_2^2 T)$ and $A_{3T} = n(2\pi)^4 / (6\bar{\kappa}_2^3 T^2)$. We calculate the second order cumulant by $\bar{\kappa}_2 = 2\pi T^{-1} \sum_{j=1}^{T-1} I_2(\omega_j) / (\psi(\bar{\boldsymbol{\vartheta}}, \omega_j) \psi(\bar{\boldsymbol{\vartheta}}, -\omega_j))$. The weights in our approach are arbitrary set as $m = 0.5$ and $n = 0.5$. Nevertheless, in [Velasco and Lobato \(2018\)](#), the weights are optimally selected depending on the magnitude of the high-order cumulants, increasing the efficiency. However, they turn out to be unintuitive and could increase the complexity of the estimation. Considering Theorem 2 in [Velasco and Lobato \(2018\)](#), we include in the spectrum and the bispectrum a consistent estimator of the standardized cumulant of orders two and three, respectively, that is

$$k_2^*(\boldsymbol{\vartheta}) = \frac{2\pi}{T} \sum_{j=1}^{T-1} \frac{I_2(\omega_j)}{\psi(\boldsymbol{\vartheta}, \omega_j)\psi(\boldsymbol{\vartheta}, -\omega_j)}, \quad k_3^*(\boldsymbol{\vartheta}) = \frac{4\pi^2}{T^2} \sum_{j=1}^{T-1} \sum_{i=1}^{T-1} \operatorname{Re} \left(\frac{I_3(\omega_j, \omega_i)}{\psi(\boldsymbol{\vartheta}, \omega_j)\psi(\boldsymbol{\vartheta}, \omega_i)\psi(\boldsymbol{\vartheta}, -\omega_j - \omega_i)} \right). \quad (31)$$

For a correct estimation and identification, the parameters and cumulants must be jointly estimated. Therefore, we use the modified spectrum and bispectrum, where the cumulants are dependent on $\boldsymbol{\vartheta}$. The modified spectrum and bispectrum are

$$S_2^*(\boldsymbol{\vartheta}, \omega_j) = S_2(\boldsymbol{\vartheta}, k_2^*(\boldsymbol{\vartheta}), \omega_j); \quad S_3^*(\boldsymbol{\vartheta}, \omega_j, \omega_i) = S_3(\boldsymbol{\vartheta}, k_3^*(\boldsymbol{\vartheta}), \omega_j, \omega_i). \quad (32)$$

Notice that the first term in $R_T(\boldsymbol{\vartheta})$ is equivalent to [Whittle \(1953\)](#) or the Gaussian-likelihood. This consistency and asymptotic normality of the estimator is developed in [Terdik \(1999\)](#); [Velasco and Lobato \(2018\)](#). The set of estimated parameters $\hat{\boldsymbol{\vartheta}}$ is obtained by minimizing R_T

$$\hat{\boldsymbol{\vartheta}} = \arg \min_{\boldsymbol{\vartheta} \in \Theta} R_T(\boldsymbol{\vartheta}), \quad (33)$$

where the parametric space Θ of $\boldsymbol{\vartheta}$ is assumed to be a subset of an Euclidean space $\mathbb{R}^{r+s+r'+s'+2}$. The global minimum is achieved if $\hat{\boldsymbol{\vartheta}} \in \Theta$, and if $R_T(\hat{\boldsymbol{\vartheta}}) \leq R_T(\boldsymbol{\vartheta}), \forall \boldsymbol{\vartheta} \in \Theta$. Note that the location of the roots outside and inside the unit circle is directly made in the transfer function in [Equation 24](#). So far, we only talked about model identifications and parameter estimations. The way the computation of the standard errors is done can be found in [Appendix A](#).

3.2 Multimodality and estimation methods

Multimodality in the estimation functions poses significant challenges when identifying and estimating noncausal and mixed models. Specifically, the presence of multiple local minima, which may closely resemble the global minimum yet reside in distinct locations, often complicates the estimation process. Conventional estimation techniques grounded in the second moment might falter in discerning between these minima. Consequently, such ambiguities can incorrectly identify noncausal models as causal and vice versa.

It's paramount to understand that multimodality is an intrinsic trait of noncausal and mixed models and not only a byproduct of the estimation methods themselves. Manifestations of multimodality are evident in MLE undertaken in both the time domain [Bec, Nielsen, and Saïdi \(2020\)](#); [Hecq et al. \(2016\)](#); [Kindop \(2021\)](#). A few potential solutions to the multimodality problem have emerged, e.g., [Cubadda, Giancaterini, Hecq, and Jasiak \(2023\)](#) proposed to use the Simulated Annealing Algorithm. Similarly, [Hecq and Velasquez-Gaviria \(2022\)](#) finds that the multimodality amplifies as the data distribution inches closer to normality and as the disparity between the roots of causal and noncausal models enlarges. Notably, multimodality can endure even for large samples.

In our context, the spectral estimation function, $R_T(\boldsymbol{\vartheta})$, presents intricate complexities. Pursuing an optimal solution via mathematical derivation becomes non-feasible given the function's topology in the parameter space Θ . This complexity is epitomized by pronounced peaks in proximity to the unit circle and steep descents as the parameter nears zero. To circumvent the challenges of multimodality and achieve precise estimations, we incorporate two optimization strategies: the Gradient Descent, and the Genetic Algorithm.

3.2.1 Gradient Descent Methods

Conventional gradient descent algorithms, such as Newton-Raphson and Nelder-Mead, may exhibit limitations when the initial values provided for optimization significantly deviate from the true values. Initial values are

usually unimportant asymptotically but important in finite samples. Consequently, there is a high likelihood of becoming trapped in a local minimum, leading to inaccurate identification and estimation of potential noncausal or mixed models. To address this concern, [Hecq and Velasquez-Gaviria \(2022\)](#) employ the computational algorithm introduced in Section 3.2 of to select an initial values that closely approximates the true set of parameters using the flipping root approach. This process can become intricate as the number of parameters increases, owing to the factorization of the characteristic function of the polynomials. Furthermore, the number of potential solutions escalates with an increasing number of parameters. To address this challenge, we use a Genetic Algorithm method.

3.2.2 Genetic Algorithm

Genetic Algorithms are a type of optimization algorithm that draws inspiration from the process of natural selection and genetics. They are widely used to address complex optimization problems. The main objective of the Genetic Algorithm is to mimic the process of evolution to iteratively search for the optimal solution in the parameter space Θ . The initial stage involves creating a population of potential solutions to the problem, representing each solution as a "chromosome" in the population. Typically, these chromosomes are encoded as binary digits (genes) strings. In the case of our study, multiple parameters that could lead to the global minimum of the estimation function $R_T(\boldsymbol{\vartheta})$ are randomly generated. Following this, all possible parameters are evaluated, and the ones that show better results are selected, resembling the survival process of living organisms. The best results are then reused in the crossover and mutation process, introducing small random changes to the parameter set in the search for the global minimum. The algorithm continues the process of selection and reproduction for a fixed number of generations or until a termination condition is met, such as the estimation function showing no significant changes. Through the iterative application of the algorithm, the entire parameter space is explored, favoring solutions with higher fitness values over time. Thus, the initial values for the estimation become irrelevant.

3.3 Identification strategy

To achieve the correct identification of the MARMA model we follow three steps.

1. We perform the Jarque-Bera to y_t (or on the residuals from the pseudo-causal model). If we reject the null hypothesis of normality, we perform steps 2 and 3. Otherwise, if the null hypothesis is not rejected, we can only estimate causal and invertible ARMA models.
2. We determine the dynamics of y_t using the ARMA(p, q) model assuming causality and invertibility. We use the AIC or BIC to select the order of p and q . In this way, there are 2^{p+q} combinations of roots that could have the same second-order probability structure. However, if y_t is non-Gaussian, only one model corresponds to the data generating process (DGP) of the data and can be found using $R_T(\boldsymbol{\vartheta})$.
3. We estimate all the combinations of MARMA(r, s, r', s') models that satisfy the order $p = r+s$ and $q = r'+s'$ using the Genetic Algorithm. The model that best fits the data emerges from the global minimum of the estimation function $R_T(\boldsymbol{\vartheta})$ of all possible models.

Example 1: Let us assume in the first step, we reject the null of Gaussianity. Then, it emerges for instance, that in the second step, we obtain the pseudo causal and invertible ARMA(2,2) model using BIC, i.e. $p = 2$ and $q = 2$. There exist nine possible MARMA(r, s, r', s') models to be estimated

Table 1: All possible MARMA(r, s, r', s') given the order $p = 2$ and $q = 2$

Model/Order	r	s	r'	s'
MARMA(2,0,2,0)	2	0	2	0
MARMA(1,1,2,0)	1	1	2	0
MARMA(0,2,2,0)	0	2	2	0
MARMA(2,0,1,1)	2	0	1	1
MARMA(1,1,1,1)	1	1	1	1
MARMA(0,2,1,1)	0	2	1	1
MARMA(2,0,0,2)	2	0	0	2
MARMA(1,1,0,2)	1	1	0	2
MARMA(0,2,0,2)	0	2	0	2

Under non-Gaussianity, and after estimating $R_T(\hat{\boldsymbol{\theta}})$ we have the following possible minima

1. There exist at least eight local minima, such as $\hat{\boldsymbol{\theta}} \in \Theta$ and $\exists \epsilon > 0$ subject to $R_T(\hat{\boldsymbol{\theta}}) \leq R_T(\boldsymbol{\theta}), \forall \boldsymbol{\theta} \in B(\hat{\boldsymbol{\theta}}, \epsilon) \cap \Theta$. where $B(\hat{\boldsymbol{\theta}}, \epsilon) := \{\boldsymbol{\theta} \mid \|\boldsymbol{\theta} - \hat{\boldsymbol{\theta}}\| \leq \epsilon\}$.
2. There exists one global minimum, such as $\hat{\boldsymbol{\theta}} \in \Theta$, and $R_T(\hat{\boldsymbol{\theta}}) \leq R_T(\boldsymbol{\theta}), \forall \boldsymbol{\theta} \in \Theta$.

Consequently, we estimate the nine models and then select the global minimum.

3.4 Estimated Residuals

To diagnose the adequacy of the estimated time-series model and do traditional inference, we first obtain the residuals in the frequency domain as follows

$$d_{\hat{\varepsilon}}(\omega) = d_T(\omega) \frac{(1 - \hat{\phi}_1^+ z - \dots - \hat{\phi}_r^+ z^r)(1 - \hat{\phi}_1^* z - \dots - \hat{\phi}_s^* z^s)}{(1 + \hat{\theta}_1^+ z + \dots + \hat{\theta}_{r'}^+ z^{r'})(1 + \hat{\theta}_1^* z + \dots + \hat{\theta}_{s'}^* z^{s'})}. \quad (34)$$

Time domain residuals $\hat{\varepsilon}_t$ are obtained by the real part of the inverse of the Fourier transform of the frequency domain residuals, as

$$\hat{\varepsilon}_t = \text{Re} \left(\frac{1}{T} \sum_{j=0}^T d_{\hat{\varepsilon}}(\omega) e^{ij\omega} \right). \quad (35)$$

Note that the methods performed directly in the time domain (see, [Hecq et al. \(2016\)](#)) must necessarily lose data due to the inclusion of initial and final conditions in terms of leads of the endogenous variable and future errors. Consequently, they generate a sequence of residuals smaller than the number of data in the time series. On the contrary, with this method, no data is lost since we work directly with the estimated coefficients and the polynomials of Equation 8. Estimate residuals will also be used for the computation of standard errors.

4 Testing for iidness

We utilize the tests recommended by [Dalla et al. \(2020\)](#) to assess the iidness of the estimated residuals. Evaluating the i.i.d assumption is important, since the incorrect beliefs about causality or invertibility might produce residuals that aren't independent, especially for orders beyond two. While these residuals might seem like white noise, they won't effectively capture key characteristics of financial returns, such as explosive trends and asymmetric cycles. On the other hand, correctly pinpointing a time series with potential noncausal or noninvertible dynamics leads to error sequences closer to the i.i.d assumption. This diminishes the necessity for models addressing heteroscedasticity, like the GARCH model (refer to [Gouriéroux et al. \(2013\)](#), [Lanne, Meitz, and Saikkonen \(2013\)](#)).

Example 1 *Let us illustrate the appearance of conditional heteroscedastic effects with a noncausal and invertible MARMA (MARMA(0,1,1,0) process) that is estimated as a traditional ARMA model. Let us consider*

$$(1 - \phi_1^* z^{-1})y_t = (1 + \theta_1^+ z)\varepsilon_t. \quad (36)$$

that has a unique and stationary representation

$$y_t = \sum_{j=-\infty}^{\infty} \Psi_j \varepsilon_{t-j}, \quad (37)$$

where Ψ_j emerges from the Laurent expansion of $(1 - \phi_1^* z^{-1})^{-1}(1 + \theta_1^+ z) \stackrel{\text{def}}{=} \Psi(z)$ and is represented by

$$\Psi_j = \begin{cases} 0 & j < 0 \\ -\frac{1}{\phi_1^*} & j = 1 \\ -\phi_1^{*-j}(1 + \theta_1^+ \phi_1^*) & j \geq 2 \end{cases}. \quad (38)$$

Assuming that ε_t has finite moments up until four, the autocorrelation function of y_t^2 is

$$\text{corr}(y_t^2, y_{t+k}^2) = \frac{(k_4^* - 3) \sum_{-\infty}^{\infty} \Psi_j^2 \Psi_{j+k}^2 + 2 \left(\sum_{-\infty}^{\infty} \Psi_j \Psi_{j+k} \right)^2}{(k_4^* - 3) \sum_{-\infty}^{\infty} \Psi_j^4 + 2 \left(\sum_{-\infty}^{\infty} \Psi_j^2 \right)^2}, \quad (39)$$

where κ_4^* is the standardized kurtosis as $k_4^* = \mathbb{E}(\varepsilon_t^4)/\sigma^4$. For $k > 1$ and non-Gaussian data, the correlation between the squares differs from zero. Equation 39 shows the apparition of heteroscedastic effects when the causal ARMA(1,1) is fitted, and the true DGP is an MARMA(0,1,1,0).

To introduce the tests of Dalla et al. (2020), we define the serial correlation, the correlation between absolute values, and the correlation between the squares, respectively as

$$\rho_{\varepsilon,k} = \text{corr}(\varepsilon_t, \varepsilon_{t-k}), \quad \rho_{|\varepsilon|,k} = \text{corr}(|\varepsilon_t|, |\varepsilon_{t-k}|), \quad \rho_{\varepsilon^2,k} = \text{corr}(\varepsilon_t^2, \varepsilon_{t-k}^2). \quad (40)$$

If ε_t is i.i.d, then $\rho_{\varepsilon,k} = \rho_{|\varepsilon|,k} = \rho_{\varepsilon^2,k} = 0$. Then, testing for iidness reduces to the absence of correlation between the levels ε_t and the absolute value $|\varepsilon_t|$, and the levels ε_t and the squares ε_t^2 . The first test is produced for individuals lags and cumulative as

$$J_{\varepsilon,|\varepsilon|,k} = \frac{T^2}{T-k} (\hat{\rho}_{\varepsilon,k}^2 + \hat{\rho}_{|\varepsilon|,k}^2), \quad C_{\varepsilon,|\varepsilon|,k} = \sum_{k=1}^m J_{\varepsilon,|\varepsilon|,k}, \quad (41)$$

with an individual lag null hypothesis, $H_0: \rho_{\varepsilon,k} = 0, \rho_{|\varepsilon|,k}$ for $k \geq 1$, and a cumulative null hypothesis, $H_0: \rho_{\varepsilon,k} = 0, \rho_{|\varepsilon|,k}$ for $k = 1, \dots, m \geq 1$. The second test is for the squares, also with individual lag and cumulative statistics

$$J_{\varepsilon,\varepsilon^2,k} = \frac{T^2}{T-k} (\hat{\rho}_{\varepsilon,k}^2 + \hat{\rho}_{\varepsilon^2,k}^2), \quad C_{\varepsilon,\varepsilon^2,k} = \sum_{k=1}^m J_{\varepsilon,\varepsilon^2,k}, \quad (42)$$

with individual lag null hypothesis, $H_0: \rho_{\varepsilon,k} = 0, \rho_{\varepsilon^2,k}$ for $k \geq 1$, and cumulative null hypothesis, $H_0: \rho_{\varepsilon,k} = 0, \rho_{\varepsilon^2,k}$ for $k = 1, \dots, m \geq 1$. If ε_t is i.i.d, the asymptotic distributions of the tests are

$$J_{\varepsilon,|\varepsilon|,k}, J_{\varepsilon,\varepsilon^2,k} \xrightarrow{D} \chi_2^2 \quad C_{\varepsilon,|\varepsilon|,k}, C_{\varepsilon,\varepsilon^2,k} \xrightarrow{D} \chi_{2m}^2 \quad \text{as } T \rightarrow \infty. \quad (43)$$

These tests have good power in the presence of dependence, conditional heteroskedasticity, or nonstationarity. Also, the χ_{2m}^2 is a good approximation for the asymptotic distribution of the test for a nonsymmetric ε_t . Similar results are obtained in McLeod and Li (1983); Wong and Ling (2005).

5 Simulation of MARMA processes

We propose a method to simulate MARMA processes in the frequency domain. Using the inverse Fourier transform, we can reconstruct the time series y_t . Unlike existing methods, i.e., [Lanne and Saikkonen \(2011\)](#), or [Hecq et al. \(2016\)](#), we do not use the representation of the series using lags and leads, with the advantage of not having to truncate their values to reach an established order. We use the transfer function in terms of its roots outside or inside the unit circle.

The steps for simulating an MARMA(r, s, r', s') are as follows

1. Simulate T realizations of an i.i.d random error sequence, that is $\{\varepsilon_t\}_{t=0}^T$, $\varepsilon_t \stackrel{\text{i.i.d}}{\sim} \mathfrak{G}(\zeta)$, and \mathfrak{G} is a distribution function, and ζ its parameters.
2. Perform the DTF of ε_t , that is $d_\varepsilon(\omega) = \sum_{t=1}^T \varepsilon_t e^{-it\omega}$.
3. Select the parameters and the orders of the MARMA(r, s, r', s') process, and create the transfer function.

$$\psi(\boldsymbol{\vartheta}, \omega) = \frac{(1 + \theta_1^+ z + \dots + \theta_{r'}^+ z^{r'})(1 + \theta_1^* z + \dots + \theta_{s'}^* z^{s'})}{(1 - \phi_1^+ z - \dots - \phi_r^+ z^r)(1 - \phi_1^* z - \dots - \phi_s^* z^s)}.$$

4. Compute the DTF of y_t as

$$d_T(\omega) = d_\varepsilon(\omega)\psi(\boldsymbol{\vartheta}, \omega).$$

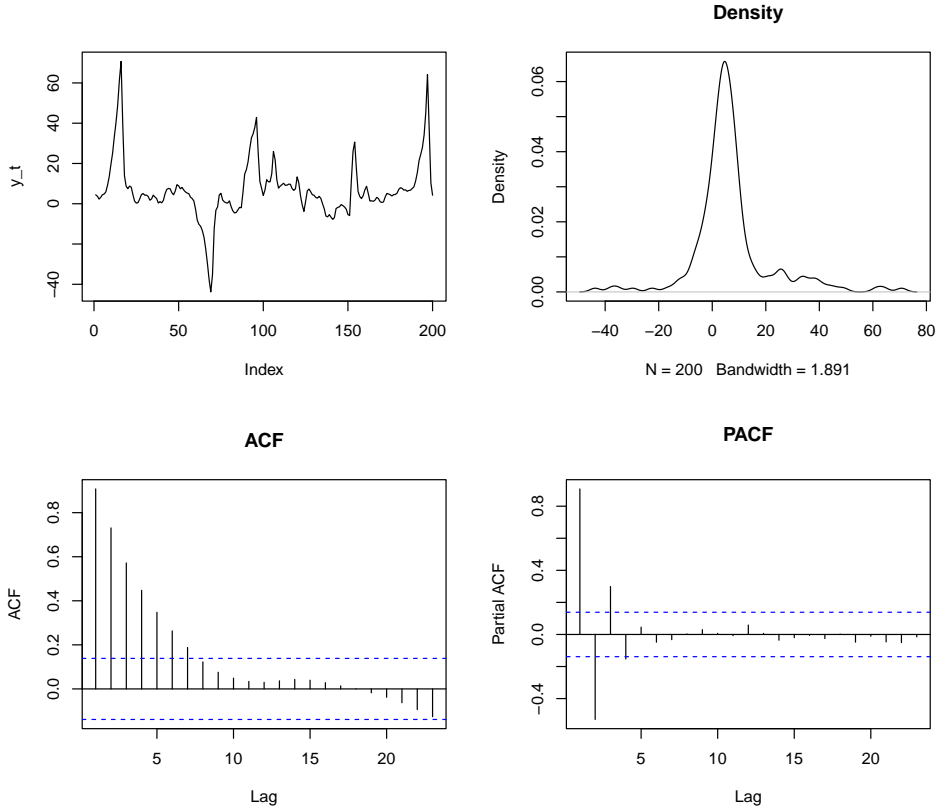
5. Recover y_t as the real part of the Inverse Fourier Transform of $d_T(\omega)$

$$y_t = \text{Re} \left(\frac{1}{T} \sum_{j=0}^T d_T(\omega) e^{ij\omega} \right).$$

To illustrate our approach we simulate an MARMA(1, 1, 1, 1) with parameters $\phi_1^+ = 0.7$, $\phi_1^* = -0.2$, $\theta_1^+ = 0.5$ and $\theta_1^* = 0.3$. The error sequence is alpha-stable $f_a(x; \alpha, \beta, \eta, \delta)$ with parameters $\alpha = 1.5$, $\beta = 0.2$, $\eta = 1$, $\delta = 0$ and $T = 200$. The pdf of the alpha-stable is introduced in Section 6. In Figure 1 we plot the trajectories of y_t , the empirical density, the ACF, and the PACF. The trajectories of the MARMA(1,1,1,1) processes are characterized by abrupt peaks or bubble phenomena, asymmetric cycles, and some short trend episodes. The ACF and PACF display patterns similar to an ARMA(2,2).

Figure 2 presents the real and imaginary part of the bispectrum and the biperiodogram of the same MARMA(1,1,1,1) process. Note that the patterns observed in the biperiodogram are replicated by the bispectrum. Also, we observe the same symmetries of the third-order cumulant in Equation 20. The white spaces imply that the relation between these frequencies is null. On the contrary, when it tends to become black, it implies a greater relation. The highest relations occur at the lowest frequencies, ω_1 , and ω_2 from 0 to 0.2 and 0.8 to 1. The relation fades as they approach the higher frequencies, from 0.4 to 0.5 and from 0.5 to 0, see [Hecq and Velasquez-Gaviria \(2022\)](#) for details.

Figure 1: Trajectory of a MARMA(1,1,1,1) alpha-stable process



6 Simulation study

We evaluate the performance of the estimator in finite samples, focusing on the correct identification and estimation of the MARMA(r, s, r', s') model. This entails discerning the causal from the noncausal autoregressive components and the invertible from the noninvertible moving average components. It should be noted that [Velasco and Lobato \(2018\)](#) conducted a simulation study for the invertible and noninvertible MA(1) model, utilizing the third and fourth-order spectral densities in the estimation. In contrast, our research centers on the MARMA models with two parameters, employing only the second and third-order spectral densities.

We focus on three type of models:

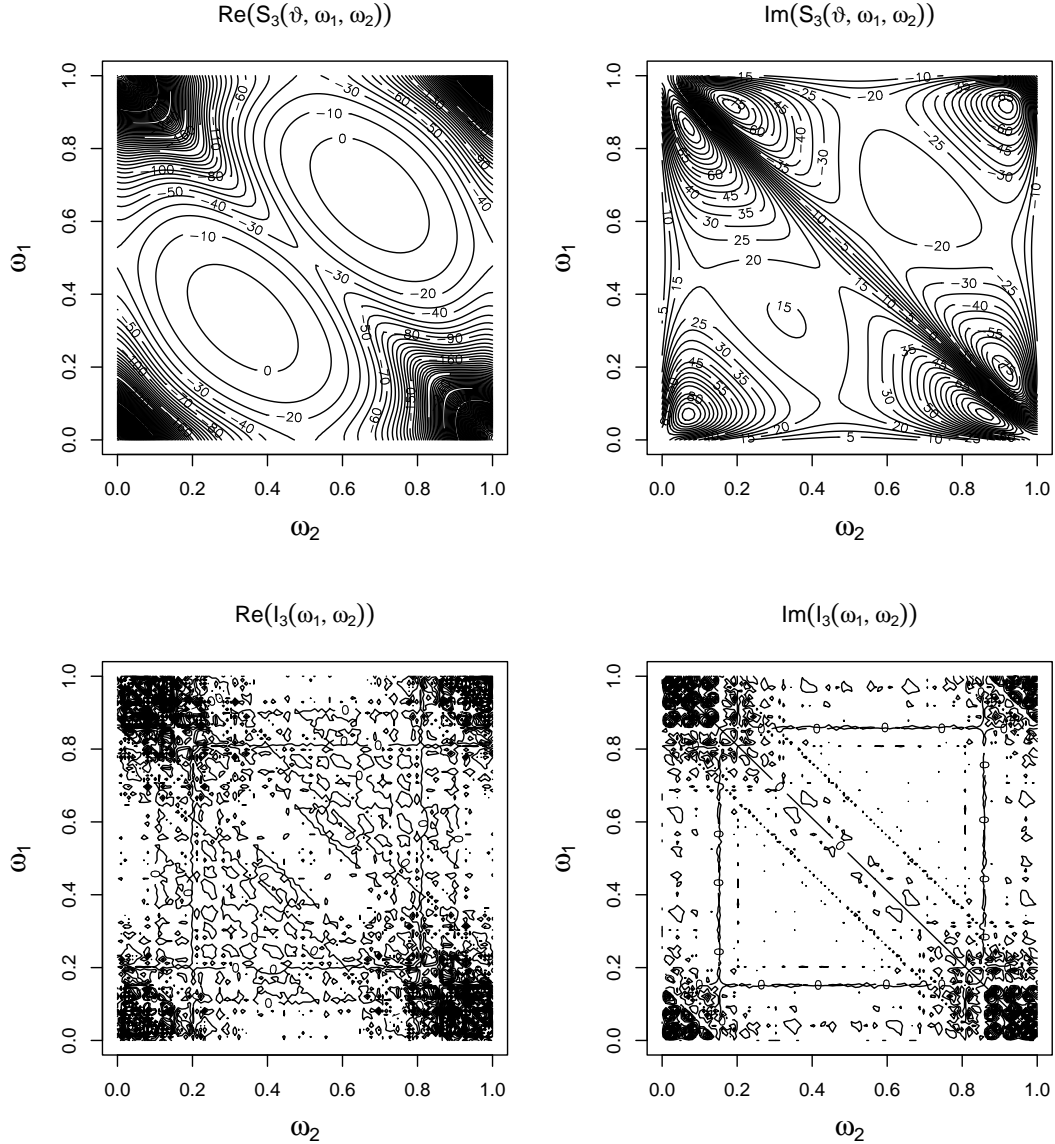
1. Autoregressive models: MAR(2,0), MAR(0,2), and MAR(1,1).
2. Moving average models: MA(2,0), MA(0,2), and MMA(1,1).
3. Combined models: MARMA(1,0,1,0), MARMA(0,1,1,0), MARMA(1,0,0,1), and MARMA(0,1,0,1).

We employ two error sequence for ε_t , that is the alpha-stable and the skew-t distribution, as proposed by [Fernández and Steel \(1998\)](#). The pdf of the alpha-stable is

$$f_a(x; \alpha, \beta, \eta, \delta) = \exp(ix\delta - |\eta x|^\alpha (1 - i\beta \operatorname{sgn}(x)(|\eta x|^{1-\alpha} - 1)\tan(\pi\alpha/2))), \quad (44)$$

where $\alpha \in (0, 2)$ is the stability parameter, $\beta \in [-1, 1]$ is the skewness parameter, $\eta > 0$ the scale parameter, and $\delta \in \mathfrak{R}$ is the location parameter. Using the alpha-stable distribution has the benefit of replicating sample features of financial returns, such as leptokurticity and skewness. However, the existence of its moments is linked to the stability parameter (α), i.e., the variance, the skewness, and the kurtosis only exist when it is equal to two. An

Figure 2: Real and Imaginary part of the bispectrum and biperiodogram for a MARMA(1,1,1,1) alpha-stable process



interesting feature of the alpha-stable distribution is its infinite divisibility, i.e., it can be expressed as a sum of i.i.d. variables while preserving its distribution. The pdf of the skew-t is

$$t_{skew}(x) = \begin{cases} \frac{2}{\gamma+1/\gamma} t(\gamma x) & \text{for } x < 0 \\ \frac{2}{\gamma+1/\gamma} t(\frac{x}{\gamma}) & \text{for } x \geq 0 \end{cases}, \quad t(x) = \frac{\Gamma(\frac{\nu+1}{2})}{\sqrt{\nu\pi}\Gamma(\frac{\nu}{2})} \left(1 + \frac{x^2}{\nu}\right)^{-(\nu+1)/2}, \quad (45)$$

where $\gamma \in \Re$ is the skewing parameter, and $t(x)$ is the pdf of the student's t distribution, where $\nu > 2$ is the degrees of freedom. The skew-t distribution can also reproduce heavy-tailed and skewed patterns. Nevertheless, its moments exist as a function of degrees of freedom. For example, the mean exists for $\nu > 1$, the variance for $\nu > 2$, the skewness for $\nu > 3$, the kurtosis for $\nu > 4$, and so forth.

For the alpha stable we consider two stability parameters $\alpha = \{1.2, 1.8\}$, one skewness parameter $\beta = 0.25$, and $\eta = 1$ and $\delta = 0$. For the skew-t, we consider two degrees of freedom $\nu = \{2, 5\}$ and skewness parameter $\gamma = 1.1$. Note that in both cases, one distribution is more leptokurtic than the other, which allows us to make comparisons

when it departs from normality to a greater extent. We also consider data lengths $T = \{100, 300, 500\}$, and a number of simulations $M = 1000$. In all cases, we report the mean estimate, the standard deviation, and the number of times the identification was correct (identification rate). Throughout the study, we employed the Genetic Algorithm for the estimation.

6.1 The MAR(r, s) DGP

We first consider the causal MAR(2,0) DGP with parameters $\phi_1^+ = 0.7$ and $\phi_2^+ = 0.2$. Then we estimate three models: a purely causal MAR(2,0), a purely noncausal MAR(0,2), and the mixed MAR(1,1). The identification rate corresponds to the frequency with which we get the correct MAR(2,0). Accordingly, the mean and standard deviation correspond to the estimated parameters of the correctly identified MAR(2,0) model in the M iterations. Subsequently, we consider as the DGP the MAR(0,2) with parameters $\phi_1^* = 0.7$ and $\phi_2^* = 0.2$, and, finally, the MAR(1,1) with parameters $\phi_1^+ = 0.7$ and $\phi_1^* = 0.2$. The same comparisons are made to establish the identification rate in both cases. We also report the mean and standard deviation of the estimated parameters. The results are presented in Table 2.

Table 2: Identification rate, the mean and standard deviation of estimated parameters of MAR(2,0), MAR(1,1), and MAR(0,2) with errors alpha-stable and skew-t

Panel A: Alpha-stable													
Dist	T	MAR(2,0)				MAR(1,1)				MAR(0,2)			
		Identification rate				Identification rate				Identification rate			
$\alpha = 1.2$	100	80%				81%				82%			
	300	94%				94%				93%			
	500	96%				96%				98%			
$\alpha = 1.8$	100	47%				55%				50%			
	300	75%				72%				77%			
	500	84%				82%				86%			
Dist	T	$\phi_1^+ = 0.7$		$\phi_2^+ = 0.2$		$\phi_1^+ = 0.7$		$\phi_1^* = 0.2$		$\phi_1^* = 0.7$		$\phi_2^* = 0.2$	
		Mean	Std	Mean	Std	Mean	Std	Mean	Std	Mean	Std	Mean	Std
$\alpha = 1.2$	100	0.721	0.135	0.153	0.118	0.670	0.123	0.203	0.136	0.713	0.117	0.172	0.120
	300	0.694	0.070	0.196	0.089	0.695	0.057	0.215	0.079	0.703	0.081	0.182	0.082
	500	0.695	0.065	0.198	0.070	0.702	0.025	0.196	0.046	0.701	0.035	0.205	0.047
$\alpha = 1.8$	100	0.734	0.130	0.127	0.140	0.665	0.132	0.211	0.165	0.736	0.118	0.150	0.128
	300	0.707	0.087	0.182	0.099	0.678	0.113	0.209	0.113	0.697	0.087	0.178	0.104
	500	0.702	0.076	0.193	0.081	0.697	0.088	0.203	0.092	0.717	0.081	0.193	0.097
Panel B: Skew t													
Dist	T	MAR(2,0)				MAR(1,1)				MAR(0,2)			
		Identification rate				Identification rate				Identification rate			
$\nu = 2$	100	68%				68%				73%			
	300	91%				74%				93%			
	500	96%				90%				95%			
$\nu = 5$	100	54%				48%				52%			
	300	62%				57%				61%			
	500	76%				65%				75%			
Dist	T	$\phi_1^+ = 0.7$		$\phi_2^+ = 0.2$		$\phi_1^+ = 0.7$		$\phi_1^* = 0.2$		$\phi_1^* = 0.7$		$\phi_2^* = 0.2$	
		Mean	Std	Mean	Std	Mean	Std	Mean	Std	Mean	Std	Mean	Std
$\nu = 2$	100	0.711	0.133	0.174	0.156	0.646	0.174	0.191	0.180	0.709	0.123	0.184	0.140
	300	0.690	0.069	0.206	0.079	0.683	0.103	0.211	0.114	0.700	0.085	0.191	0.093
	500	0.707	0.050	0.206	0.062	0.693	0.051	0.194	0.067	0.696	0.063	0.196	0.068
$\nu = 5$	100	0.732	0.146	0.168	0.179	0.613	0.167	0.222	0.217	0.746	0.131	0.133	0.161
	300	0.719	0.085	0.186	0.130	0.673	0.101	0.207	0.132	0.679	0.115	0.220	0.132
	500	0.711	0.078	0.198	0.084	0.687	0.084	0.202	0.122	0.703	0.090	0.191	0.096

6.2 The MMA(r', s') DGP

We first consider the invertible MA(2,0) with parameters $\theta_1^+ = 0.7$ and $\theta_2^+ = 0.2$. Then we estimate the model assuming invertibility, noninvertibility MA(0,2), and mixed MMA(1,1). The identification rate corresponds to the number of times the estimation resulted in the invertible model MA(2,0). The mean and standard deviation

correspond to the estimated parameters of the MA(2,0) model in the M iterations. We next consider as DGP the noninvertible MA(0,2) with parameters $\theta_1^* = 0.7$ and $\theta_2^* = 0.2$, and finally the MAR(1,1) with parameters $\theta_1^+ = 0.7$ and $\theta_1^* = 0.2$. The same comparisons are made to establish identification rates and statistics on estimated parameters. The results are presented in Table 3.

Table 3: Identification rate, the mean and standard deviation of estimated parameters of MA(2,0), MMA(1,1), and MA(0,2) with errors alpha-stable and skew-t

Panel A: Alpha-stable													
Dist	T	MA(2,0)				MMA(1,1)				MA(0,2)			
		Identification rate				Identification rate				Identification rate			
$\alpha = 1.2$	100	96%				74%				92%			
	300	98%				81%				96%			
	500	99%				86%				98%			
$\alpha = 1.8$	100	66%				52%				64%			
	300	80%				69%				82%			
	500	87%				76%				88%			
Dist	T	$\theta_1^+ = 0.7$		$\theta_2^+ = 0.2$		$\theta_1^+ = 0.7$		$\theta_1^* = 0.2$		$\theta_1^* = 0.7$		$\theta_2^* = 0.2$	
		Mean	Std	Mean	Std	Mean	Std	Mean	Std	Mean	Std	Mean	Std
$\alpha = 1.2$	100	0.709	0.081	0.197	0.128	0.674	0.251	0.168	0.160	0.650	0.199	0.178	0.133
	300	0.705	0.053	0.209	0.059	0.728	0.108	0.171	0.095	0.686	0.099	0.200	0.074
	500	0.701	0.035	0.199	0.041	0.709	0.087	0.201	0.065	0.693	0.052	0.202	0.048
$\alpha = 1.8$	100	0.725	0.137	0.217	0.116	0.698	0.111	0.192	0.156	0.670	0.115	0.188	0.122
	300	0.695	0.111	0.195	0.114	0.716	0.107	0.174	0.127	0.707	0.073	0.215	0.074
	500	0.710	0.076	0.204	0.071	0.706	0.095	0.209	0.077	0.703	0.047	0.205	0.063

Panel B: Skew t													
Dist	T	MA(2,0)				MMA(1,1)				MA(0,2)			
		Identification rate				Identification rate				Identification rate			
$\nu = 2$	100	88%				76%				80%			
	300	91%				80%				95%			
	500	93%				87%				98%			
$\nu = 5$	100	58%				59%				52%			
	300	68%				65%				68%			
	500	71%				76%				82%			
Dist	T	$\theta_1^+ = 0.7$		$\theta_2^+ = 0.2$		$\theta_1^+ = 0.7$		$\theta_1^* = 0.2$		$\theta_1^* = 0.7$		$\theta_2^* = 0.2$	
		Mean	Std	Mean	Std	Mean	Std	Mean	Std	Mean	Std	Mean	Std
$\nu = 2$	100	0.686	0.108	0.186	0.103	0.682	0.105	0.187	0.139	0.669	0.092	0.203	0.128
	300	0.694	0.080	0.194	0.084	0.722	0.104	0.188	0.084	0.680	0.081	0.187	0.079
	500	0.697	0.076	0.202	0.067	0.702	0.091	0.194	0.079	0.686	0.063	0.202	0.059
$\nu = 5$	100	0.683	0.109	0.204	0.122	0.678	0.159	0.215	0.161	0.656	0.112	0.159	0.110
	300	0.686	0.062	0.194	0.092	0.679	0.117	0.213	0.098	0.688	0.068	0.188	0.070
	500	0.697	0.060	0.201	0.061	0.689	0.074	0.205	0.071	0.692	0.056	0.203	0.057

6.3 The MARMA(r, s, r', s') DGP

For the MARMA, the DGP is first the causal and invertible model MARMA(1,0,1,0), that is $p = 1$ and $q = 1$, with parameters $\phi_1^+ = 0.7$ and $\theta_1^* = 0.2$. We then estimate the model assuming causality and invertibility MARMA(1, 0, 1, 0), noncausality and invertibility MARMA(0,1,1,0), causality and noninvertibility MARMA(1, 0, 0, 1) and finally noncausality and noninvertibility MARMA(0, 1, 0, 1). Subsequently, we consider as DGP the noncausal and invertible model MARMA(0, 1, 1, 0) with parameters $\phi_1^* = 0.7$ and $\theta_1^+ = 0.2$, then the causal and noninvertible model MARMA(1,0,0,1) with parameters $\phi_1^+ = 0.7$ and $\theta_1^* = 0.2$, and finally the noncausal and noninvertible model MARMA(0,1,0,1) with parameters $\phi_1^* = 0.7$ and $\theta_1^+ = 0.2$. The same comparisons are made to establish the identification rate in all cases. In each case, we report the mean and standard deviation of the estimated parameters. The results are presented in Table 4.

6.4 Monte Carlo outcomes

In Tables 2, 3, it is obvious that the model identification is a function of the level at which the data depart from normality. For example, for the alpha-stable distribution with $\alpha = 1.2$ and the skew-t with $\nu = 2$, the

Table 4: Identification rate, the mean and standard deviation of estimated parameters of the MARMA(1,0,1,0), MARMA(0,1,1,0), MARMA(1,0,0,1), and MARMA(0,1,0,1) with errors alpha-stable and skew-t

Panel A: Alpha-stable																	
Dist	T	MARMA(1,0,1,0)				MARMA(0,1,1,0)				MARMA(1,0,0,1)				MARMA(0,1,0,1)			
		Identification rate				Identification rate				Identification rate				Identification rate			
$\alpha = 1.2$	100	78%				80%				84%				88%			
	300	92%				98%				98%				92%			
	500	96%				99%				98%				95%			
$\alpha = 1.8$	100	54%				47%				48%				51%			
	300	61%				70%				70%				63%			
	500	74%				82%				78%				75%			
Dist	T	$\phi_1^+ = 0.7$		$\theta_1^+ = 0.2$		$\phi_1^* = 0.7$		$\theta_1^* = 0.2$		$\phi_1^+ = 0.7$		$\theta_1^+ = 0.2$		$\phi_1^* = 0.7$		$\theta_1^* = 0.2$	
		Mean	Std	Mean	Std	Mean	Std	Mean	Std	Mean	Std	Mean	Std	Mean	Std	Mean	Std
$\alpha = 1.2$	100	0.666	0.118	0.209	0.150	0.703	0.061	0.189	0.099	0.682	0.095	0.205	0.096	0.674	0.076	0.225	0.106
	300	0.708	0.040	0.212	0.104	0.699	0.041	0.203	0.049	0.701	0.042	0.210	0.069	0.696	0.043	0.187	0.099
	500	0.700	0.035	0.196	0.094	0.701	0.032	0.200	0.047	0.700	0.038	0.201	0.045	0.704	0.039	0.197	0.057
$\alpha = 1.8$	100	0.680	0.078	0.243	0.162	0.667	0.109	0.223	0.170	0.709	0.095	0.169	0.182	0.706	0.087	0.211	0.185
	300	0.691	0.065	0.214	0.131	0.689	0.053	0.206	0.085	0.697	0.054	0.217	0.100	0.693	0.052	0.196	0.100
	500	0.702	0.039	0.198	0.073	0.693	0.050	0.203	0.080	0.705	0.041	0.208	0.076	0.708	0.039	0.205	0.081

Panel B: Skew t																	
Dist	T	MARMA(1,0,1,0)				MARMA(0,1,1,0)				MARMA(1,0,0,1)				MARMA(0,1,0,1)			
		Identification rate				Identification rate				Identification rate				Identification rate			
$\nu = 2$	100	65%				64%				69%				64%			
	300	84%				81%				86%				80%			
	500	90%				86%				96%				88%			
$\nu = 5$	100	42%				56%				66%				51%			
	300	58%				61%				73%				58%			
	500	71%				68%				88%				70%			
Dist	T	$\phi_1^+ = 0.7$		$\theta_1^+ = 0.2$		$\phi_1^* = 0.7$		$\theta_1^* = 0.2$		$\phi_1^+ = 0.7$		$\theta_1^+ = 0.2$		$\phi_1^* = 0.7$		$\theta_1^* = 0.2$	
		Mean	Std	Mean	Std	Mean	Std	Mean	Std	Mean	Std	Mean	Std	Mean	Std	Mean	Std
$\nu = 2$	100	0.708	0.086	0.187	0.143	0.693	0.096	0.185	0.141	0.673	0.128	0.205	0.167	0.669	0.145	0.212	0.179
	300	0.699	0.050	0.202	0.097	0.698	0.082	0.211	0.086	0.698	0.057	0.200	0.097	0.682	0.061	0.209	0.103
	500	0.696	0.046	0.203	0.086	0.700	0.043	0.193	0.076	0.702	0.047	0.201	0.077	0.704	0.053	0.201	0.086
$\nu = 5$	100	0.692	0.091	0.193	0.168	0.712	0.128	0.159	0.209	0.682	0.132	0.207	0.170	0.662	0.156	0.212	0.185
	300	0.694	0.059	0.198	0.093	0.701	0.063	0.206	0.095	0.699	0.055	0.198	0.128	0.696	0.071	0.205	0.099
	500	0.699	0.052	0.201	0.079	0.700	0.054	0.205	0.079	0.702	0.036	0.197	0.080	0.699	0.063	0.199	0.085

identification rate is significantly higher than in the case of $\alpha = 1.8$ and $\nu = 5$, being the latter close to the normal distribution, with thinner tails. In all cases, the identification rate increases as T increases. Note that when the $T = 100$ for $\alpha = 1.8$ and $\nu = 5$, the identification is close to 50%. This indicates that the model cannot be accurately identified. The empirical bias of the estimated parameters and the standard deviation also depends on the leptokurticity of the generated data. As it departs from normality, there is less bias and less standard deviation. In addition, the empirical bias and standard deviation decrease as T increases. For the AR and MA components, the 0.2 parameter has a larger bias than the 0.7 parameter. Table 4 exhibits a correct estimation and identification of the MARMA model, both for the AR and the MA components, regardless of the location of the roots, outside or inside the unit circle. For the four models, the identification is similar.

7 Empirical application

7.1 Data description

We consider monthly returns of 24 Famma-French emerging market stocks portfolios observed from January 1990 to August 2022, for a total of 392 months. The data set is taken from Kenneth French's website http://mba.tuck.dartmouth.edu/pages/faculty/ken.french/data_library.html. The emerging markets countries currently included are Argentina, Brazil, Chile, China, Colombia, Czech Republic, Egypt, Greece, Hungary, India, Indonesia, Malaysia, Mexico, Pakistan, Peru, Philippines, Poland, Qatar, Russia, Saudi Arabia, South Africa, South Korea, Taiwan, Thailand, Turkey, United Arab Emirates.

All returns are in U.S. dollars, include dividends and capital gains, and are not continuously compounded.

We consider several categories of returns. In the first category, the stocks are sorted by two Market-cap (size) and three book-to-market equity (B/M) groups, leading to six average value-weighted portfolios. The returns of the portfolios are in Figure 3. Big-size stocks are those in the country’s top 90% of the market cap, and small stocks are those in the bottom 10%. The B/M breakpoints for big and small stocks in a country are the 30th and 70th percentiles of B/M for the big stocks of the country. In the second category, the stocks are sorted by two sizes and three profitability (OP) groups, leading to six average value-weighted portfolios. The returns of the portfolios are in Figure 4. The OP breakpoints for big and small stocks in a country are the 30th and 70th percentiles of OP for the big stocks of the country. In the third category, the stocks are sorted by two sizes and three Investment (Inv) groups, leading to six average value-weighted portfolios, The returns of the portfolios are in Figure 5. The Inv breakpoints for big and small stocks in a country are the 30th and 70th percentiles of Inv for the big stocks of the country. In the fourth category, the stocks are sorted by two market sizes and three lagged momentum return groups (MOM), leading to six average value-weighted portfolios, The returns of the portfolios are in Figure 6. For portfolios formed at the end of the month $t-1$, the lagged momentum return is a stock’s cumulative return for $t-12$ to $t-2$. The momentum breakpoints for all stocks in a country are the 30th and 70th percentiles of the lagged momentum returns of the country’s big stocks.

We selected the portfolios in emerging markets since the dynamics are stronger than those found in developed markets, as they are exposed to a greater extent to risk factors such as interest rate variations, currency devaluation, and policy changes between governments, among others. For an application in developed markets, see [Gospodinov and Ng \(2015\)](#) where all portfolios exhibit noninvertible MA(0,1) dynamics.

7.2 Data features

Although the constructed portfolios are formed from assets in competitive markets and are diversified among different countries and sectors, they exhibit characteristics of time dependency that MARMA models can capture. In addition, the portfolios exhibit non-Gaussian characteristics such as skewness and kurtosis, which we can observe in Table 5.

We perform a preliminary estimation of ARMA models by Gaussian-likelihood to select lag orders, assuming consequently causality and invertibility. To identify the dynamics, we rely on the BIC, the significance of the lags in the ACF and the PACF, as well as the significance of the coefficients in each possible model. We restrict the order of the AR component to $p = 2$ and the MA component to $q = 2$. In Table 5, we report the mean, the standard deviation, the skewness, the kurtosis, and the identification of the ARMA model using Gaussian-likelihood estimation.

Table 5: Descriptive Statistics and Dynamics

	Size and Book-to-Market Portfolios				
	Mean	Sd.Dev.	Skewness	Kurtosis	Dynamics
Small Size and Low B/M	0.005	0.067	-0.107	6.095	AR(2)
Medium Size 1 and B/M 2	0.010	0.062	-0.408	5.017	AR(2)
Small size and High B/M	0.014	0.063	-0.233	4.846	AR(2)
Big Size and Low B/M	0.007	0.059	-0.461	4.795	AR(2)
Medium Size 2 and B/M 2	0.009	0.063	-0.584	4.955	AR(2)
Big Size and High B/M	0.010	0.066	-0.366	4.633	AR(1)
	Size and Operating Profitability Portfolios				
	Mean	Sd.Dev.	Skewness	Kurtosis	Dynamics
Small Size and Low OP	0.008	0.061	-0.492	5.147	AR(2)
Medium Size 1 and OP 2	0.011	0.059	-0.488	5.142	AR(2)
Small Size and High OP	0.009	0.060	-0.611	4.981	AR(2)
Big Size and Low OP	0.006	0.066	-0.401	4.768	AR(2)
Medium Size 2 and OP 2	0.007	0.061	-0.668	5.513	AR(2)
Big Size and High OP	0.009	0.060	-0.519	4.386	AR(2)
	Size and Investment Portfolios				
	Mean	Sd.Dev.	Skewness	Kurtosis	Dynamics
Small Size and Low INV	0.010	0.061	-0.434	4.849	AR(2)
Medium Size 1 and INV 2	0.011	0.059	-0.537	5.125	AR(2)
Small Size and High INV	0.007	0.065	-0.477	5.340	AR(2)
Big Size and Low INV	0.009	0.059	-0.529	4.583	AR(2)
Medium Size 2 and INV 2	0.008	0.061	-0.592	5.195	AR(2)
Big Size and High INV	0.007	0.067	-0.526	5.202	AR(2)
	Size and Momentum Portfolios				
	Mean	Sd.Dev.	Skewness	Kurtosis	Dynamics
Small Size and Low MOM	0.004	0.066	-0.041	6.162	AR(1)
Medium Size 1 and MOM 2	0.012	0.059	-0.514	5.571	AR(2)
Small Size and High MOM	0.013	0.062	-0.549	4.641	AR(2)
Big Size and Low MOM	0.004	0.067	-0.256	5.481	AR(2)
Medium Size 2 and MOM 2	0.008	0.061	-0.542	5.138	AR(1)
Big Size and high MOM	0.011	0.061	-0.687	4.793	AR(2)

Overall the mean of the returns is close to zero. The standard deviations are in the range of 0.059 and 0.067, in annual terms between 20% and 23%. All portfolios have negative skewness and excess kurtosis. The low B/M, low OP, and low MOM portfolios display higher kurtosis than the high B/M, high OP, and high MOM portfolios. On the contrary, the low INV portfolio has a lower kurtosis than the high INV portfolio. It is found that all returns follow autoregressive processes without a moving average component. Out of twenty-four portfolios, twenty-one are AR(2), and three are AR(1).

7.3 MARMA identification

Table 6 reports the estimation using $R_T(\theta)$. We present the identified models as well as the estimated parameters with the standard errors computed as in Appendix A. The tests for i.i.d and the p -value for the first five lags of the Ljung-Box test are reported in Table 7.

We found noncausal features in all of the twenty-four portfolios. This result indicates that these portfolios have the characteristic of adjusting adequately to near future events by creating expectations of the prices of the assets that compose them. They anticipate the impact that new information entering into the market may have.

No moving average dynamics were detected. In eleven cases, the model identification was MAR(1,1). In ten cases, MAR(0,2) and MAR(0,1) in three cases. No correlation exists between the residuals, as shown in Table 7. In nineteen portfolios, we do not reject the null hypothesis of zero correlation for the test between the levels and squares of the errors. This means there are no remaining traces of GARCH effects in the residuals. In contrast, we rejected the null hypothesis of no correlation between the levels and the absolute value of the residuals on fifteen occasions.

Size and Book-to-Market Portfolios: For the small size and low B/M portfolio, we identify an MAR(1,1).

However, we reject the null hypothesis for the absolute value and squares tests. The model found in the second portfolio, Medium Size 1 and B/M 2, is an MAR(1,1). For the residuals of this model, the null hypothesis in absolute value and squares is not rejected. The Small size and High B/M portfolio is an MAR(1,1). In this case, the null hypothesis is not rejected for the absolute value. However, lag number two is significant at 5% but not at the 10% significance level. We do not reject the null hypothesis for any lag in the squares. The Big Size and Low B/M portfolio is an MAR(1,1). We do not reject the null hypothesis in any test. The Medium Size 2 and B/M 2 portfolio is an MAR(0,2). In this case, we do not reject the null hypothesis for the first lag of the absolute value. However, we reject it after that. On the other hand, we do not reject the null hypothesis for the squares. The Big Size and High B/M portfolio is MAR(0,1). We reject the null hypothesis for the absolute value and do not reject the null hypothesis for the squares.

Size and Operating Profitability Portfolios: The Small Size and Low OP portfolio is an MAR(1,1). For both tests, the null hypothesis is not rejected. The Medium Size 1 and OP 2 portfolio is MAR(1,1). The null hypothesis is rejected for the absolute value but not rejected for the squares. The Small Size and High OP portfolio is an MAR(1,1). The null hypothesis is not rejected for the two tests, however, lags two and three of the absolute value test are marginally significant at 5% but not at 10%. The Big Size and Low OP portfolio is an MAR(0,2). In this case, the null hypothesis is not rejected for the squares test. However, the null hypothesis is rejected for lags three onwards in the absolute value test. The Medium Size 2 and OP 2 and Big Size and High OP portfolios are also MAR(0,2). However, we reject the null hypothesis in the absolute value test for lag two onwards. In the test of squares, we do not reject the null hypothesis.

Size and Investment Portfolios: The portfolios Small Size and Low INV and Medium Size 1 and INV 2 are MAR(1,1). We do not reject the null hypothesis at any lag for both tests. The Small Size and High INV portfolio is also an MAR(1,1), although we reject the null hypothesis in the absolute value test for lags two onwards. The Big Size and Low INV portfolio is MAR(0,2), and the null hypothesis is not rejected for both tests. On the other hand, the portfolios Medium Size 2 and INV 2 and Big Size and High INV are MAR(0,2). We do not reject the null hypothesis for the test of squares. However, we reject the null hypothesis for the absolute value test.

Size and Momentum Portfolios: The Small Size and Low MOM portfolio is an MAR(0,1). On the other hand, the Medium Size 1 and MOM 2 and Small Size and High MOM portfolios are MAR(0,2). We reject the null hypothesis in the absolute value and squares tests for these three portfolios. The Big Size and Low MOM portfolio is an MAR(1,1), the Medium Size 2 and MOM 2 portfolio is an MAR(0,1), and the Big Size and high MOM portfolio is an MAR(0,2). For the residuals of the three portfolios, we reject the null hypothesis in the absolute value test for all lags. Conversely, we do not reject the null hypothesis in the test of squares.

Table 6: Estimation of portfolios returns using $R_T(\vartheta)$

<i>Size and Book-to-Market Portfolios</i>	Model	Causal		Noncausal	
		ϕ_1^+	ϕ_2^+	ϕ_1^*	ϕ_2^*
Small Size and Low B/M	MAR(1,1)	-0.368 (0.046)		0.506 (0.049)	
Medium Size 1 and B/M 2	MAR(1,1)	-0.154 (0.046)		0.438 (0.051)	
Small Size and High B/M	MAR(1,1)	-0.191 (0.052)		0.434 (0.047)	
Big Size and Low B/M	MAR(1,1)	-0.222 (0.051)		0.429 (0.047)	
Medium Size 2 and B/M 2	MAR(0,2)			0.168 (0.051)	0.154 (0.051)
Big Size and High B/M	MAR(0,1)			0.242 (0.051)	
<i>Size and Operating Profitability Portfolios</i>	Model	ϕ_1^+	ϕ_2^+	ϕ_1^*	ϕ_2^*
Small Size and Low OP	MAR(1,1)	-0.125 (0.053)		0.455 (0.048)	
Medium Size 1 and OP 2	MAR(1,1)	-0.186 (0.053)		0.461 (0.048)	
Small Size and High OP	MAR(1,1)	-0.155 (0.053)		0.405 (0.049)	
Big Size and Low OP	MAR(0,2)			0.199 (0.053)	0.120 (0.053)
Medium Size 2 and OP 2	MAR(0,2)			0.205 (0.052)	0.163 (0.053)
Big Size and High OP	MAR(0,2)			0.177 (0.053)	0.141 (0.053)
<i>Size and Investment Portfolios</i>	Model	ϕ_1^+	ϕ_2^+	ϕ_1^*	ϕ_2^*
Small Size and Low INV	MAR(1,1)	-0.138 (0.053)		0.417 (0.054)	
Medium Size 1 and INV 2	MAR(1,1)	-0.185 (0.053)		0.486 (0.048)	
Small Size and High INV	MAR(1,1)	-0.153 (0.054)		0.464 (0.048)	
Big Size and Low INV	MAR(0,2)			0.193 (0.053)	0.111 (0.054)
Medium Size 2 and INV 2	MAR(0,2)			0.180 (0.053)	0.160 (0.054)
Big Size and High INV	MAR(0,2)			0.229 (0.053)	0.132 (0.054)
<i>Size and Momentum Portfolios</i>	Model	ϕ_1^+	ϕ_2^+	ϕ_1^*	ϕ_2^*
Small Size and Low MOM	MAR(0,1)			0.286 (0.051)	
Medium Size 1 and MOM 2	MAR(0,2)			0.251 (0.051)	0.110 (0.052)
Small Size and High MOM	MAR(0,2)			0.229 (0.051)	0.107 (0.052)
Big Size and Low MOM	MAR(1,1)	-0.212 (0.051)		0.406 (0.048)	
Medium Size 2 and MOM 2	MAR(0,1)			0.213 (0.051)	
Big Size and high MOM	MAR(0,2)			0.187 (0.051)	0.139 (0.052)

Table 7: Ljung-Box, $C_{\varepsilon,|\varepsilon|}$ and $C_{\varepsilon,\varepsilon^2}$ tests p-values

Portfolios	Ljung-Box lags					$C_{\varepsilon, \varepsilon }$ lags					$C_{\varepsilon,\varepsilon^2}$ lags				
	1	2	3	4	5	1	2	3	4	5	1	2	3	4	5
Size and Book-to-Market															
Small Size and Low B/M	0.286	0.171	0.279	0.413	0.537	0.000	0.000	0.000	0.000	0.000	0.000	0.000	0.000	0.000	0.000
Medium Size 1 and B/M 2	0.619	0.877	0.958	0.975	0.991	0.482	0.400	0.564	0.663	0.487	0.495	0.826	0.955	0.988	0.988
Small Size and High B/M	0.600	0.438	0.624	0.754	0.827	0.534	0.027	0.050	0.097	0.130	0.488	0.265	0.469	0.675	0.814
Big Size and Low B/M	0.343	0.518	0.711	0.691	0.809	0.264	0.104	0.051	0.082	0.086	0.184	0.229	0.317	0.443	0.629
Medium Size 2 and B/M 2	0.628	0.288	0.407	0.392	0.495	0.052	0.027	0.005	0.001	0.002	0.263	0.201	0.152	0.161	0.281
Big Size and High B/M	0.193	0.366	0.513	0.596	0.709	0.047	0.003	0.003	0.003	0.006	0.098	0.157	0.279	0.372	0.546
Size and Operating Profitability															
Small Size and Low OP	0.232	0.420	0.561	0.703	0.769	0.197	0.218	0.370	0.497	0.395	0.184	0.432	0.659	0.828	0.902
Medium Size 1 and OP 2	0.180	0.178	0.304	0.439	0.565	0.101	0.018	0.038	0.064	0.029	0.085	0.099	0.217	0.388	0.519
Small Size and High OP	0.456	0.623	0.804	0.872	0.860	0.057	0.036	0.046	0.074	0.011	0.086	0.218	0.379	0.573	0.526
Big Size and Low OP	0.860	0.551	0.749	0.778	0.690	0.286	0.224	0.064	0.013	0.019	0.341	0.377	0.393	0.403	0.468
Medium Size 2 and OP 2	0.669	0.355	0.558	0.539	0.636	0.063	0.028	0.018	0.002	0.003	0.274	0.277	0.346	0.318	0.477
Big Size and High OP	0.500	0.262	0.355	0.362	0.409	0.261	0.042	0.004	0.001	0.002	0.427	0.119	0.073	0.079	0.139
Size and Investment															
Small Size and Low INV	0.286	0.305	0.498	0.665	0.775	0.128	0.083	0.127	0.221	0.134	0.259	0.370	0.545	0.750	0.867
Medium Size 1 and INV 2	0.321	0.579	0.778	0.851	0.928	0.184	0.187	0.391	0.415	0.271	0.128	0.376	0.642	0.793	0.893
Small Size and High INV	0.266	0.342	0.504	0.654	0.705	0.128	0.027	0.036	0.077	0.035	0.058	0.085	0.203	0.375	0.419
Big Size and Low INV	0.460	0.294	0.334	0.384	0.371	0.265	0.083	0.142	0.056	0.088	0.398	0.309	0.376	0.463	0.533
Medium Size 2 and INV 2	0.672	0.224	0.381	0.499	0.459	0.120	0.036	0.006	0.001	0.002	0.267	0.178	0.169	0.232	0.300
Big Size and High INV	0.410	0.346	0.548	0.606	0.743	0.009	0.003	0.000	0.000	0.001	0.084	0.059	0.083	0.088	0.181
Size and Momentum															
Small Size and Low MOM	0.381	0.587	0.784	0.876	0.928	0.001	0.000	0.000	0.000	0.000	0.000	0.001	0.003	0.007	0.007
Medium Size 1 and MOM 2	0.505	0.788	0.924	0.933	0.971	0.002	0.001	0.002	0.003	0.003	0.009	0.027	0.082	0.158	0.231
Small Size and High MOM	0.398	0.390	0.597	0.756	0.864	0.001	0.000	0.000	0.000	0.000	0.002	0.004	0.012	0.023	0.032
Big Size and Low MOM	0.835	0.183	0.326	0.482	0.625	0.161	0.003	0.003	0.007	0.014	0.122	0.054	0.052	0.112	0.207
Medium Size 2 and MOM 2	0.243	0.351	0.532	0.626	0.760	0.010	0.001	0.001	0.001	0.001	0.109	0.067	0.077	0.138	0.263
Big Size and high MOM	0.464	0.764	0.891	0.589	0.530	0.337	0.078	0.031	0.003	0.003	0.239	0.414	0.493	0.341	0.410

8 Conclusions

In this study, we introduced a novel estimation method for MARMA models that may contain both causal and non-causal components, as well as invertible and non-invertible elements. Our approach relies on the spectrum, bispectrum, periodogram, and biperiodogram. Instead of leveraging the i.i.d. nature of residuals as many methods do, we utilize high-order cumulants. The proposed estimation function yields unbiased parameters and displays an asymptotic normal distribution. It consistently identifies the underlying data-generating process, particularly when the data shows deviations from normality. For this identification, it's crucial for the third and fourth moments/cumulants to be non-zero. Our claims are backed by comprehensive Monte Carlo simulations using the alpha-stable and skew-t distribution.

Additionally, we introduce a simulation technique for MARMA processes that utilizes the Fourier transform of the error sequence and the transfer function. This method stands out because it avoids the AR or MA representation of the stationary MARMA solution. As a result, no data is lost due to the need for an initial or final condition, and it eliminates potential bias from using lead variables and future errors.

When conducting estimations in the frequency domain, errors can still be extracted in the time domain using the inverse Fourier transform. We suggest three tests on these residuals to assess their potential dependence structures and gauge how closely they align with the i.i.d. assumption.

Lastly, we applied our methods to an empirical dataset comprising 24 monthly returns of Fama-French stock portfolios from emerging markets. We identified a mix of causal, non-causal, and purely non-causal dynamics. This result indicates that these portfolios have the characteristic of adjusting adequately to near future events by creating expectations of the prices of the assets that compose them. They anticipate the impact that new information entering into the market may have. This feature is especially valuable from the point of view of risk management and portfolio construction.

The calculated residuals consistently resembled white noise without any heteroscedastic effects. In contrast, estimating using the conventional AR process, which assumes causality, did produce white noise residuals. However, these also showed heteroscedastic effects, suggesting a need for a GARCH model.

References

- Alekseev, V. (1996). Asymptotic properties of higher-order periodograms. *Theory of Probability & Its Applications*, 40(3), 409–419.
- Bartelt, H., Lohmann, A. W., & Wirtzner, B. (1984). Phase and amplitude recovery from bispectra. *Applied optics*, 23(18), 3121–3129.
- Bartlett, M. S. (1950). Periodogram analysis and continuous spectra. *Biometrika*, 37(1/2), 1–16.
- Bec, F., Nielsen, H. B., & Saïdi, S. (2020). Mixed causal–noncausal autoregressions: Bimodality issues in estimation and unit root testing 1. *Oxford Bulletin of Economics and Statistics*, 82(6), 1413–1428.
- Breid, F. J., Davis, R. A., Lh, K.-S., & Rosenblatt, M. (1991). Maximum likelihood estimation for noncausal autoregressive processes. *Journal of Multivariate Analysis*, 36(2), 175–198.
- Breidt, F., & Davis, R. (1992). Time-reversibility, identifiability and independence of innovations for stationary time series. *Journal of Time Series Analysis*, 13(5), 377–390.
- Brillinger, D. R. (1975). Time series. data analysis and theory. holt, renehart and winston. *Inc., New York*.

- Brillinger, D. R. (1985). Fourier inference: Some methods for the analysis of array and nongaussian series data 1. *JAWRA Journal of the American Water Resources Association*, 21(5), 743–756.
- Brillinger, D. R., & Rosenblatt, M. (1967). Asymptotic theory of estimates of kth-order spectra. *Proceedings of the National Academy of Sciences of the United States of America*, 57(2), 206.
- Brockwell, P. J., & Davis, R. A. (1987). *Time series: theory and methods*. Springer-Verlag. New York.
- Cubadda, G., Giancaterini, F., Hecq, A., & Jasiak, J. (2023). Optimization of the generalized covariance estimator in noncausal processes. *arXiv preprint arXiv:2306.14653*.
- Dalla, V., Giraitis, L., & Phillips, P. C. (2020). Robust tests for white noise and cross-correlation. *Econometric Theory*, 1–29.
- Diba, B. T., & Grossman, H. I. (1988). The theory of rational bubbles in stock prices. *The Economic Journal*, 98(392), 746–754.
- Fama, E. F. (1970). Efficient capital markets: A review of theory and empirical work. *The journal of Finance*, 25(2), 383–417.
- Fernández, C., & Steel, M. F. (1998). On bayesian modeling of fat tails and skewness. *Journal of the american statistical association*, 93(441), 359–371.
- Fischer, S. (1977). Long-term contracts, rational expectations, and the optimal money supply rule. *Journal of political economy*, 85(1), 191–205.
- Fries, S. (2021). Conditional moments of noncausal alpha-stable processes and the prediction of bubble crash odds. *Journal of Business & Economic Statistics*, 1–21.
- Gospodinov, N., & Ng, S. (2015). Minimum distance estimation of possibly noninvertible moving average models. *Journal of Business & Economic Statistics*, 33(3), 403–417.
- Gouriéroux, C., & Zakoïan, J.-M. (2017). Local explosion modelling by non-causal process. *Journal of the Royal Statistical Society: Series B (Statistical Methodology)*, 79(3), 737–756.
- Gouriéroux, C., Zakoïan, J.-M., et al. (2013). *Explosive bubble modelling by noncausal process*. CREST.
- Hansen, L. P., Sargent, T. J., et al. (1991). Two difficulties in interpreting vector autoregressions. *Rational expectations econometrics*, 1, 77–119.
- Hecq, A., Lieb, L., & Telg, S. (2016). Identification of mixed causal-noncausal models in finite samples. *Annals of Economics and Statistics/Annales d'Économie et de Statistique*(123/124), 307–331.
- Hecq, A., & Velasquez-Gaviria, D. (2022). Spectral estimation for mixed causal-noncausal autoregressive models. *arXiv preprint arXiv:2211.13830*.
- Hecq, A., & Voisin, E. (2019). Predicting bubble bursts in oil prices during the covid-19 pandemic with mixed causal-noncausal models. *arXiv preprint arXiv:1911.10916*.
- Huang, J., & Pawitan, Y. (2000). Quasi-likelihood estimation of non-invertible moving average processes. *Scandinavian Journal of Statistics*, 27(4), 689–702.
- Kay, S. M., & Marple, S. L. (1981). Spectrum analysis—a modern perspective. *Proceedings of the IEEE*, 69(11), 1380–1419.
- Kindop, I. (2021). Ubiquitous multimodality in mixed causal-noncausal processes.
- Kumon, M. (1992). Identification of non-minimum phase transfer function using higher-order spectrum. *Annals of the Institute of Statistical Mathematics*, 44(2), 239–260.

- Lanne, M., Meitz, M., & Saikkonen, P. (2013). Testing for linear and nonlinear predictability of stock returns. *Journal of financial econometrics*, 11(4), 682–705.
- Lanne, M., & Saikkonen, P. (2011). Noncausal autoregressions for economic time series. *Journal of Time Series Econometrics*, 3(3).
- Leonenko, N. N., Sikorskii, A. Y., & Terdik, G. (1998). On spectral and bispectral estimator of the parameter of nongaussian data.
- Lii, K., & Rosenblatt, M. (1982). Deconvolution and estimation of transfer function phase and coefficients for nongaussian linear processes: The annals of statistics, v. 10.
- Lii, K.-S., & Rosenblatt, M. (1992). An approximate maximum likelihood estimation for non-gaussian non-minimum phase moving average processes. *Journal of Multivariate Analysis*, 43(2), 272–299.
- Lii, K.-S., & Rosenblatt, M. (1996). Maximum likelihood estimation for nongaussian nonminimum phase arma sequences. *Statistica Sinica*, 1–22.
- Lobato, I. N., & Velasco, C. (2022). Single step estimation of arma roots for nonfundamental nonstationary fractional models. *The Econometrics Journal*, 25(2), 455–476.
- Lof, M. (2013). Noncausality and asset pricing. *Studies in Nonlinear Dynamics and Econometrics*, 17(2), 211–220.
- Lof, M., & Nyberg, H. (2017). Noncausality and the commodity currency hypothesis. *Energy Economics*, 65, 424–433.
- Lucas Jr, R. E. (1972). Expectations and the neutrality of money. *Journal of economic theory*, 4(2), 103–124.
- McLeod, A. I., & Li, W. K. (1983). Diagnostic checking arma time series models using squared-residual autocorrelations. *Journal of time series analysis*, 4(4), 269–273.
- Meitz, M., & Saikkonen, P. (2013). Maximum likelihood estimation of a noninvertible arma model with autoregressive conditional heteroskedasticity. *Journal of Multivariate Analysis*, 114, 227–255.
- Muth, J. F. (1961). Rational expectations and the theory of price movements. *Econometrica: Journal of the Econometric Society*, 315–335.
- Nyholm, J., et al. (2019). Essays on noninvertible arma models.
- Rosenblatt, M. (1965). *Stationary sequences and random fields*. Springer Science & Business Media.
- Rosenblatt, M. (1980). Linear processes and bispectra. *Journal of Applied Probability*, 17(1), 265–270.
- Rosenblatt, M. (2000). *Gaussian and non-gaussian linear time series and random fields*. Springer Science & Business Media.
- Rosenblatt, M. (2012). *Random processes* (Vol. 17). Springer Science & Business Media.
- Shiller, R. J., Fischer, S., & Friedman, B. M. (1984). Stock prices and social dynamics. *Brookings papers on economic activity*, 1984(2), 457–510.
- Terdik, G. (1999). *Bilinear stochastic models and related problems of nonlinear time series analysis: a frequency domain approach* (Vol. 142). Springer Science & Business Media.
- Velasco, C. (2022). Estimation of time series models using residuals dependence measures. *The Annals of Statistics*, 50(5), 3039–3063.
- Velasco, C., & Lobato, I. N. (2018). Frequency domain minimum distance inference for possibly nonin-

vertible and noncausal arma models. *The Annals of Statistics*, 46(2), 555–579.

Whittle, P. (1953). Estimation and information in stationary time series. *Arkiv för matematik*, 2(5), 423–434.

Wong, H., & Ling, S. (2005). Mixed portmanteau tests for time-series models. *Journal of Time Series Analysis*, 26(4), 569–579.

Wu, R., & Davis, R. A. (2010). Least absolute deviation estimation for general autoregressive moving average time-series models. *Journal of Time Series Analysis*, 31(2), 98–112.

Appendix A: Asymptotic Variance

Holding Theorem 1 and 3 in [Velasco and Lobato \(2018\)](#), the asymptotic normality of the second and third-order estimator can be expressed as

$$\sqrt{T} \left(\hat{\vartheta} - \vartheta_0 \right) \rightarrow N(0, \mathbb{W}).$$

The matrix \mathbb{W} stands for the asymptotic variance

$$\mathbb{W} = \begin{bmatrix} (\Phi_0 + \Phi_0^*)^{-1} & \Phi_0^{-1} \\ \Phi_0^{-1} & \frac{v_4+2}{v_3^2} \Phi_0^{-1} + \Phi_0^{-1} \Phi_0^* \Phi_0^{-1} \end{bmatrix},$$

where, $v_4 = \frac{\kappa_4}{\kappa_2^2}$ stands for the standardized kurtosis, $v_3 = \frac{\kappa_3}{\kappa_2^{3/2}}$ stands for the standardized skewness, and

$$\Phi_0 = \frac{1}{2\pi} \int_{-\pi}^{\pi} \psi^1(\vartheta_0; \omega) \psi^1(\vartheta_0; -\omega)' d\omega; \quad \Phi_0^* = \frac{1}{2\pi} \int_{-\pi}^{\pi} \psi^1(\vartheta_0; \omega) \psi^1(\vartheta_0; \omega)' d\omega,$$

where $\psi^1(\vartheta_0; \omega) = \psi(\vartheta_0; \omega) - \mu(\vartheta_0)$, $\psi(\vartheta_0; \omega) = \frac{\partial}{\partial \vartheta} \log \psi(\vartheta_0; \omega)$, and $\mu(\vartheta_0) = \frac{1}{2\pi} \int_{-\pi}^{\pi} \psi(\vartheta_0; \omega) d\omega$. To prove the existence of $\mu(\vartheta_0)$, one needs to exclude the unit root case. This integral is different from 0 only when the model is noninvertible. The matrix Φ_0 is positive definite, excluding unit and common roots in the MA and AR polynomials. For the second order estimation the asymptotic variance is $\mathbb{W}_{1,1} = (\Phi_0 + \Phi_0^*)^{-1}$. For the third order estimation is $\mathbb{W}_{2,2} = \frac{v_4+2}{v_3^2} \Phi_0^{-1} + \Phi_0^{-1} \Phi_0^* \Phi_0^{-1}$.

For an MA(1,0), the transfer function is $\psi(\vartheta_0; \omega) = 1 + \theta_1^+ e^{i\omega}$. The FOC respect with the parameter is

$$\varphi(\vartheta_0; \omega) = \frac{\partial}{\partial \vartheta} \log \left(1 + \theta_1^+ e^{i\omega} \right) = \frac{e^{i\omega}}{1 + \theta_1^+ e^{i\omega}},$$

and

$$\varphi(\vartheta_0; -\omega) = \frac{e^{-i\omega}}{1 + \theta_1^+ e^{-i\omega}}.$$

The centering parameters can be found by the Cauchy formula as

$$\mu(\vartheta_0, \omega) = \frac{1}{2\pi} \int_{-\pi}^{\pi} \frac{e^{i\omega}}{1 + \theta_1^+ e^{i\omega}} d\omega = \begin{cases} \frac{1}{\theta_1^+} & |\theta_1^+| > 1 \\ 0 & \text{if } \frac{1}{|\theta_1^+|} \neq 1, \end{cases}$$

$$\mu(\vartheta_0, -\omega) = \frac{1}{2\pi} \int_{-\pi}^{\pi} \frac{e^{-i\omega}}{1 + \theta_1^+ e^{-i\omega}} d\omega = \begin{cases} \frac{1}{\theta_1^+} & |\theta_1^+| \geq 1 \\ 0 & \text{if } \frac{1}{|\theta_1^+|} \neq 1. \end{cases}$$

Then

$$\varphi^1(\vartheta_0, \omega) = \frac{e^{i\omega}}{1 + \theta_1^+ e^{i\omega}}; \quad \varphi^1(\vartheta_0, -\omega) = \frac{e^{-i\omega}}{1 + \theta_1^+ e^{-i\omega}}.$$

In this sense,

$$\Phi_0 = \frac{1}{2\pi} \int_{-\pi}^{\pi} \frac{e^{i\omega}}{1 + \theta_1^+ e^{i\omega}} \frac{e^{-i\omega}}{1 + \theta_1^+ e^{-i\omega}} d\omega = \frac{1}{1 - \theta_1^{+2}}, \text{ and } \Phi_0^* = \frac{1}{2\pi} \int_{-\pi}^{\pi} \frac{e^{i\omega}}{1 + \theta_1^+ e^{i\omega}} \frac{e^{i\omega}}{1 + \theta_1^+ e^{i\omega}} d\omega = 0.$$

For other MARMA models, the procedure is straightforward. [Lobato and Velasco \(2022\)](#) present closed forms for the standard errors, greatly simplifying the inference.

Figures

Figure 3: Size and B/M portfolios

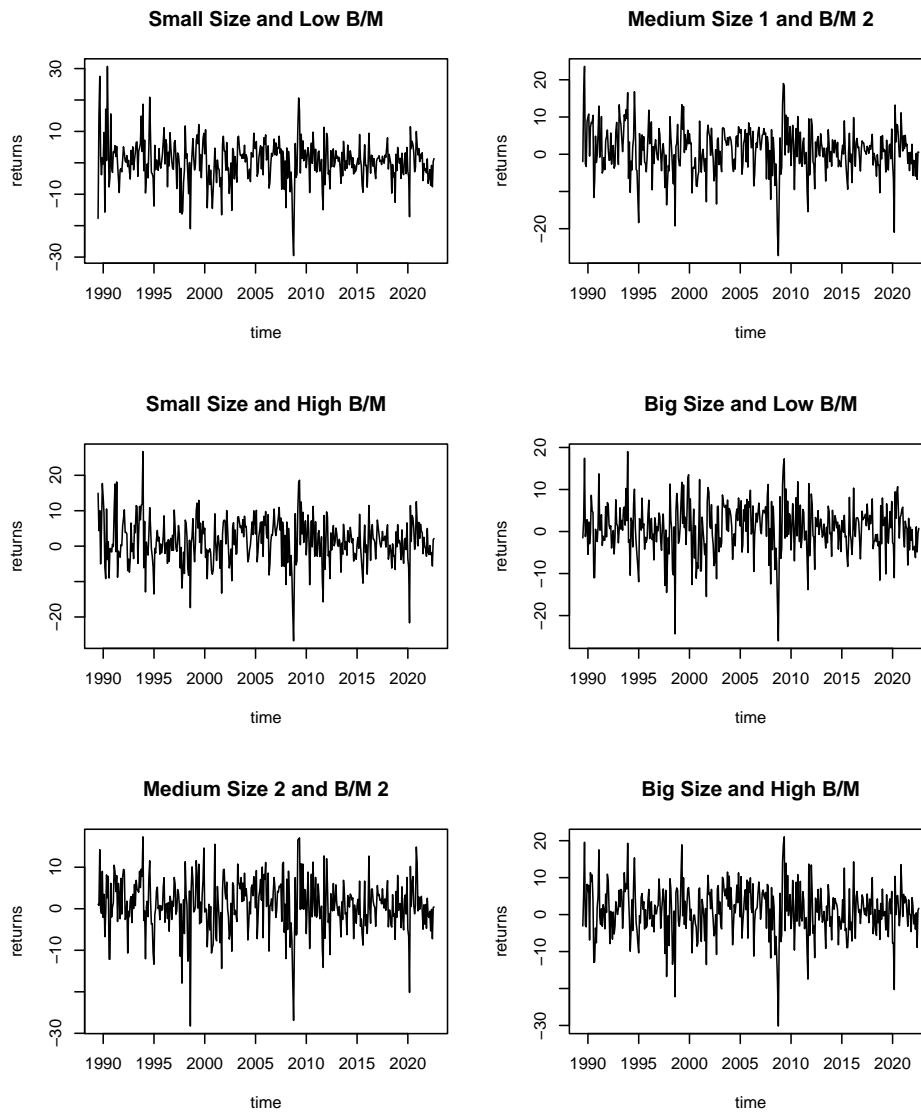


Figure 4: Size and Operating Profit portfolios

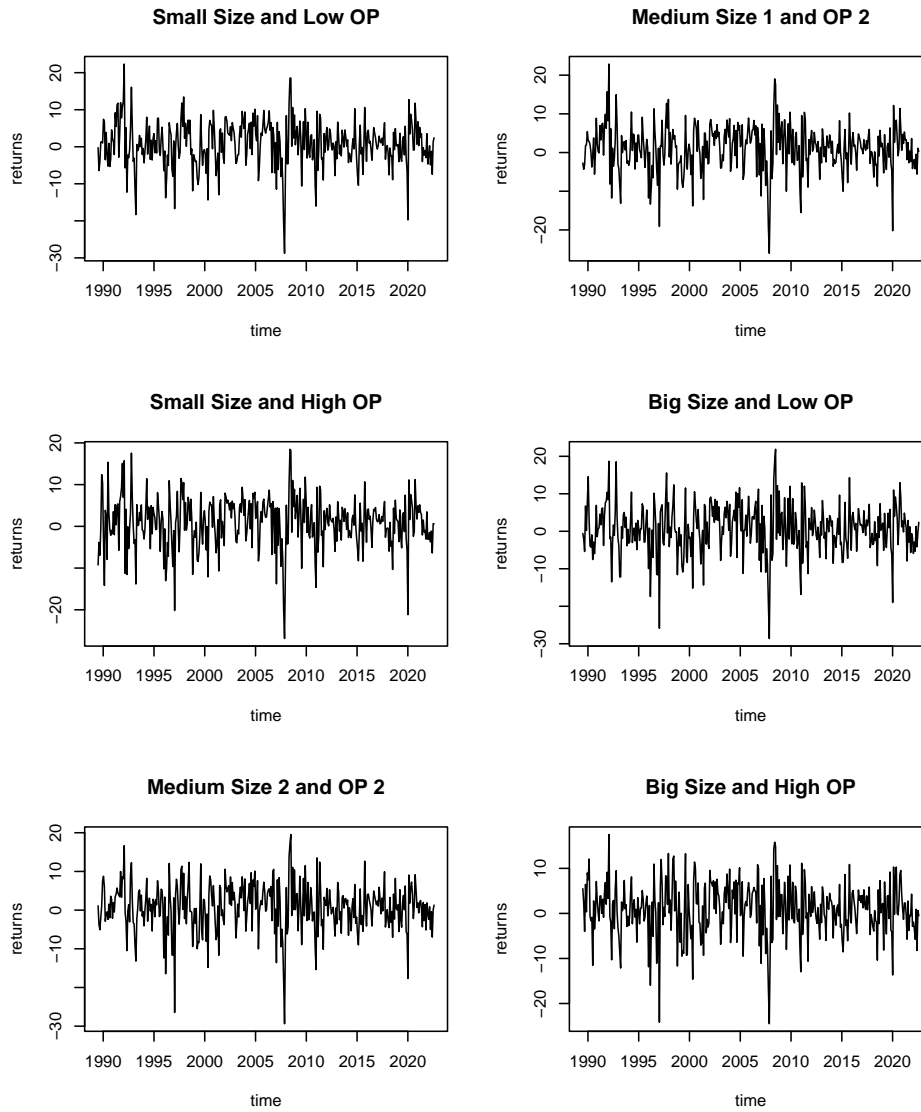


Figure 5: Size and Investment portfolios

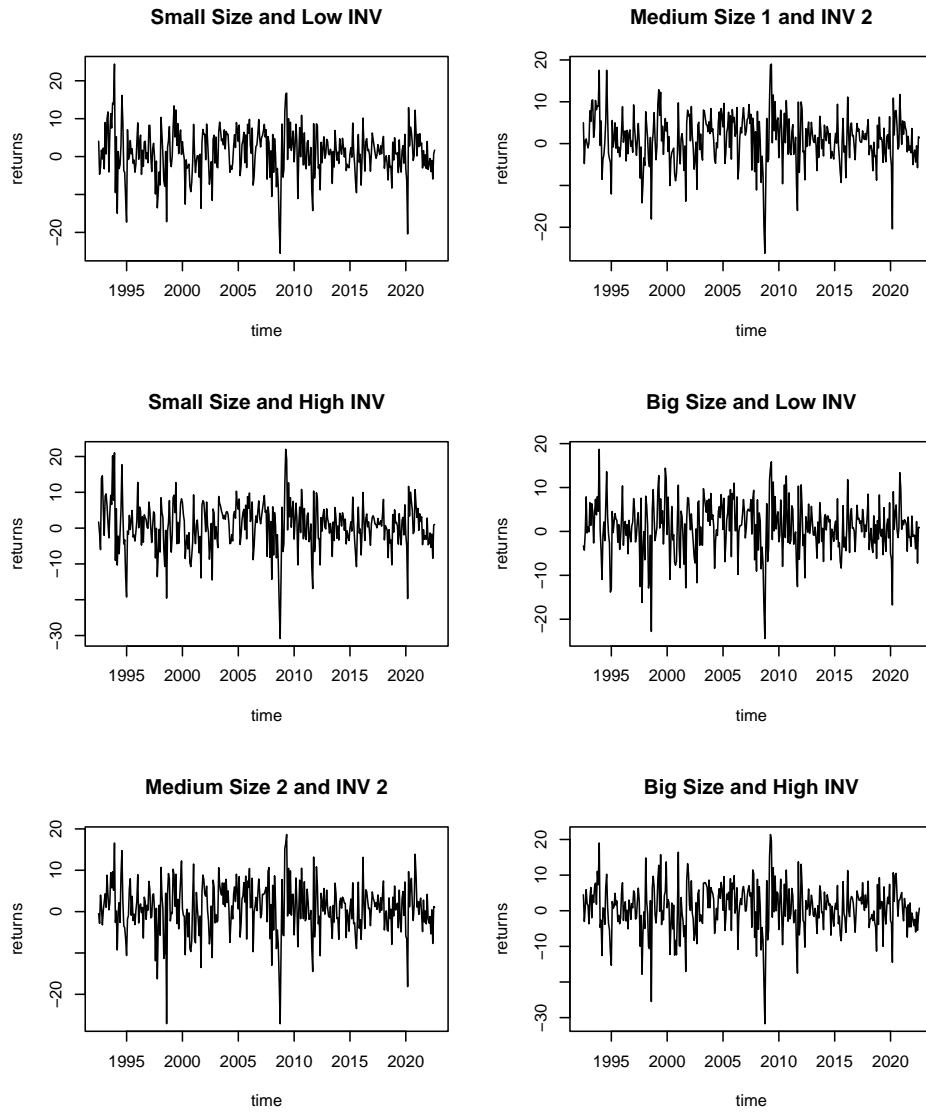


Figure 6: Size and Momentum portfolios

